ICARUS 66, 579–609 (1986)

The Gas Composition of Jupiter Derived from 5-μm Airborne Spectroscopic Observations

GORDON L. BJORAKER[1] AND HAROLD P. LARSON

Lunar and Planetary Laboratory, University of Arizona, Tucson, Arizona 85721

AND

VIRGIL G. KUNDE

Laboratory for Extraterrestrial Physics, Goddard Space Flight Center, Greenbelt, Maryland 20771

Received November 25, 1985; revised March 11, 1986

The atmospheric transmission window between 1850 and 2250 cm^{-1} in Jupiter's atmosphere was observed at a spectral resolution of 0.5 cm^{-1} from the Kuiper Airborne Observatory. The mole fractions of NH_3, PH_3, CH_4, CH_3D, CO, and GeH_4 were derived for the 1- to 6-bar portion of Jupiter's troposphere using a spectrum synthesis program. Knowledge of the abundances of these gases below the visible clouds is necessary to calculate the global inventory of nitrogen, phosphorus, carbon, and deuterium, which, in turn, may constrain models of Jupiter's formation. The N/H ratio is 1.5 ± 0.2 times the value for the Sun's photosphere. The P/H ratio for the 5-bar level is between 1.0 and 1.6 times the solar abundance. The weak $\nu_3 - \nu_4$ hot band of CH_4 was detected for the first time on Jupiter, thus providing a deep atmospheric value for C/H of 3.6 ± 1.2 times solar. The Jovian deuterium abundance is comparable to that measured in the interstellar medium (D/H = 1.2 ± 0.5) × 10^{-5}. CO appears to be well mixed with a mole fraction of (1.0 ± 0.3) × 10^{-9}. Multiple absorption features confirm that GeH_4 is present on Jupiter with a mole fraction of $(7.0^{+4.0}_{-2.0}) \times 10^{-10}$. The observed abundances of CO, GeH_4, and PH_3 are consistent with models of convective transport from Jupiter's deep atmosphere.

1. INTRODUCTION

Jupiter's 5-μm spectrum is a very diagnostic observational tool to probe the troposphere of this giant planet. The low opacity at 5 μm of the principal gaseous absorbers H_2 and CH_4 and the low particulate opacity in selected "Hot Spot" regions allow us to see deeper into Jupiter's atmosphere in this spectral region than at any other wavelength from the ultraviolet (λ = 0.10 μm) to the microwave (λ = 10 cm). The presence of strong vibration–rotation bands at 5 μm for many gases, combined with long path lengths and higher tropospheric temperatures, permits the detection of trace quantities of a number of molecules in Jupiter's atmosphere. Knowledge of the abundances of these gases below Jupiter's visible clouds is useful as a description of the present state of the upper envelope of this planet's atmosphere, and it also serves to indicate various physical and chemical processes that occur on Jupiter.

In this paper we report abundance analyses of NH_3, PH_3, CH_4, CH_3D, CO, and GeH_4 in the 1- to 6-bar pressure range in Jupiter's troposphere. All of these molecules have been previously detected in ground-based, airborne, and spacecraft observations of Jupiter (Beer and Taylor, 1973; Beer, 1975; Ridgway *et al.*, 1976; Larson *et al.*, 1977; Beer and Taylor, 1978a,b; Larson *et al.*, 1978; Fink *et al.*, 1978; Kunde *et al.*, 1982; Drossart *et al.*, 1982). The new contribution of this study is a self-consistent simultaneous determination of the abundances of all of these molecules at the same physical level in Jupiter's atmosphere using one high spectral resolution dataset and a radiative transfer model. Water vapor is also a key molecule in Jupiter's

[1] Now a NAS/NRC Resident Research Associate at NASA/GSFC.

0019-1035/86 $3.00

atmosphere (Larson *et al.*, 1975; Drossart and Encrenaz, 1982; Kunde *et al.*, 1982); we analyze its abundance and distribution in a separate publication (Bjoraker *et al.*, 1986a).

Jovian 5-μm absorbers can be divided into three categories to emphasize their role as tracers of physics and chemistry in Jupiter's atmosphere. The abundance of CH_4, NH_3, H_2O, and CH_3D at deep levels provides us with a measure of the total inventory of carbon, nitrogen, oxygen, and deuterium in Jupiter. Comparing these elemental and isotopic abundances with the solar atmosphere may constrain models of Jupiter's formation from the solar nebula. Two of the molecules listed above, NH_3 and H_2O, condense to form clouds in Jupiter's troposphere. Knowledge of their abundances below the clouds determines the cloud mass and the pressure level where condensation takes place. Finally, three additional gases, PH_3, CO, and GeH_4, are not expected to be detectable at all in the upper troposphere. Their presence can best be explained by rapid vertical transport from great depths. Phosphine may also serve as a tracer of the oxidation state of the deep atmosphere. Phosphorus, in the form of P_4 derived photochemically from PH_3, may be responsible for the yellow and red colors observed in the clouds present in Jupiter's belts and in the Great Red Spot.

2. OBSERVATIONS

We used two observational datasets in this study. One consists of high-resolution observations of Jupiter at 5 μm from the Kuiper Airborne Observatory (KAO). The other consists of spatially resolved measurements of Jupiter's belts and zones using the Infrared Interferometer Spectrometer and Radiometer (IRIS) on Voyager 1. This dataset covers the thermal infrared spectrum from 4.5 to 50 μm. We used the 4.5- to 5.5-μm portion of this spectrum in which thermal radiation originates at levels between 1 and 6 bars in Jupiter's troposphere. This combination of spectroscopic data at high spectral resolution with broadband observations at high spatial resolution provides a wealth of information about processes in Jupiter's troposphere. In this paper we use the KAO data almost exclusively, while in companion papers (Bjoraker *et al.*, 1986a,b) we focus on the IRIS data.

The airborne observations were acquired with a rapid-scanning Fourier spectrometer (Larson and Fink, 1975) on the 90-cm telescope aboard the KAO. The spectrum is an average of observations on the nights of 1975 December 10, 12, and 13 UT of the central 25″ of the 41.4″ disk of Jupiter. This average includes all Jovian longitudes from $-40°$ to $+40°$ latitude. The average spectrum has a peak signal to rms noise ratio of about 100 and a spectral resolution of 0.5 cm^{-1}.

We used the Voyager IRIS data and an airborne lunar comparison spectrum to place the airborne planetary spectrum on an absolute radiance scale. The high-altitude spectrum of the Moon at 5 μm was recorded with the same spectrometer used for the Jupiter observations at a comparable airmass. The ratio JUPITER/MOON removes both telluric spectral features and the wavelength dependent response of the spectrometer from the planetary data. Thermal emission of the Moon, however, must be removed by ratioing the lunar spectrum to a black body whose temperature must be determined. Thermal modeling of the infrared brightness temperature of the Moon (Saari *et al.*, 1972) indicates that the observed temperature varies rapidly with solar elevation angle in a range between 200 and 350 K. Our airborne lunar observations were near the terminator; consequently, the uncertainty in the 5-μm lunar brightness temperature for our viewing geometry is large.

We therefore employed a technique using the absolutely calibrated Voyager IRIS data to calculate this temperature. We selected 1703 pre-encounter IRIS spectra whose

field of view on Jupiter closely matched that observed from the KAO. The airborne data were smoothed to the 4.3-cm^{-1} Voyager resolution for a direct comparison. The positions and strengths of Jovian absorption features in both datasets were in excellent agreement. The slope of the continuum in the JUPITER/(MOON/Black Body) spectrum depends, of course, on the choice of black-body temperature. We adjusted this temperature until the airborne data matched the IRIS observations. The best fit was for a lunar brightness temperature of 240 K, consistent with the permissible range in Saari *et al.* The accuracy of this method depends on the assumption that, averaged over all longitudes for the −40° to +40° latitude range, Jupiter's 5-μm spectrum was the same in March 1979 as in December 1975. Terrile and Beebe (1979) showed that at small spatial scales Jupiter's appearance at 5 μm changed considerably during this time. For our central disk observations, however, the assumption of time-independent 5-μm flux should be reasonable. The final calibrated airborne spectrum of Jupiter is shown at the full 0.5-cm^{-1} resolution in Fig. 1.

3. RADIATIVE TRANSFER TECHNIQUES

Our procedure for interpreting Jupiter's infrared spectrum at 5 μm consists of generating a synthetic spectrum from a radiative transfer model, comparing it to

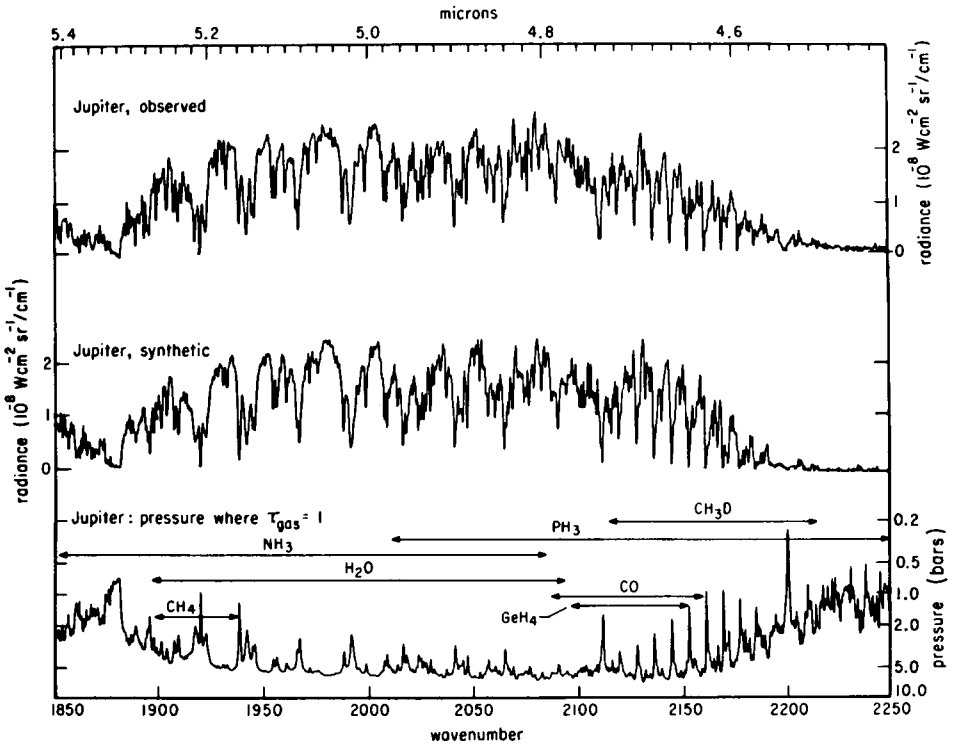

FIG. 1. Jupiter's 5-μm spectrum observed from the KAO (top) is compared with the best synthetic spectrum (center) generated using a radiative transfer model. The observed spectrum is an average over all longitudes of the −40 to 40° latitude region in December 1975. Absorption lines of gaseous NH_3, PH_3, H_2O, CH_4, CH_3D, CO, and GeH_4 are formed in the troposphere between 1 and 6 bars. The gas mole fractions used to calculate the center spectrum are summarized in Table VI. The lower trace indicates the atmospheric pressure levels where the gas optical depth equals unity. The maximum contribution to the emergent radiation originates from this level. Pressure induced absorption by H_2 limits the depth of penetration to about 6 bars in the most transparent portions of the 5-μm window.

the observed airborne data, and iterating parameters in the model atmosphere until the synthetic spectrum agrees with the observations within error limits. We used a spectrum synthesis program developed by Kunde and Maguire (1974). This algorithm computes the monochromatic absorption spectrum by numerically summing the contributions of many individual molecular absorption lines. The average transmittance between each of 35 layers and the top of the atmosphere is computed for frequency intervals which are smaller than the pressure broadened linewidths. The emergent radiance is calculated at 0.1-cm^{-1} intervals. This spectrum is then convolved with the instrument function at a resolution of 0.5 cm^{-1} for comparison with the airborne data.

Several parameters serve as input to this program. First, a temperature—pressure profile of Jupiter's atmosphere is specified. Figure 2 displays the profile obtained by inversion of far infrared radiances of Jupiter using IRIS data (Kunde *et al.*, 1982). The temperature at 1 bar is 165 K (Lindal *et al.*, 1981) and the dashed line is an adiabatic extrapolation to deeper levels. We calculated the adiabatic lapse rate using a hydrogen mole fraction of 0.897 (Gautier *et al.*, 1981) taking into account the variation of the specific heat of H_2 with temperature. The hydrogen and helium mole fractions were prescribed (Gautier *et al.*, 1981), while the mole fractions of the other seven gases were left as adjustable parameters. These gases are NH_3, PH_3, CH_4, CH_3D, CO, GeH_4, and H_2O. Finally, the program reads in a molecular line atlas containing absorption line positions, strengths, and lower state energies for the wavelength interval of interest; the spectroscopic parameters for each Jovian absorber are described in the Appendix. The output is a synthetic spectrum which is then compared to the observed spectrum. The mole fractions of the gases listed above were iterated until an acceptable fit was obtained.

The shapes of the absorption lines were described by collisionally broadened Lorentz profiles. Accurate knowledge of the far-wing lineshape of pressure-broadened infrared absorbers is needed to model Jupiter's 5-μm spectrum adequately. Unfortunately, this lineshape is poorly understood (Kunde, 1982). We approximated the sub-Lorentz behavior of the far-wing lineshape by using a Lorentz profile in a specified frequency interval symmetric about the line center; beyond this range we set the absorption coefficient to zero. Our Lorentz cutoff parameter is therefore independent of temperature and pressure. Other authors have adopted different criteria. Gautier *et al.* (1982) specified the Lorentz cutoff in terms of an integral number of half widths of each molecule. Using this approach the cutoff parameter has the same functional form as the Lorentz half width: it varies proportionally with the pressure and with the inverse of the square root of the temperature. Thus, estimates of the Lorentz cutoff parameter range from 30 cm^{-1} at 1 bar and 300 K for the ν_4 band of CH_4 (Gautier *et al.*, 1982) to a constant

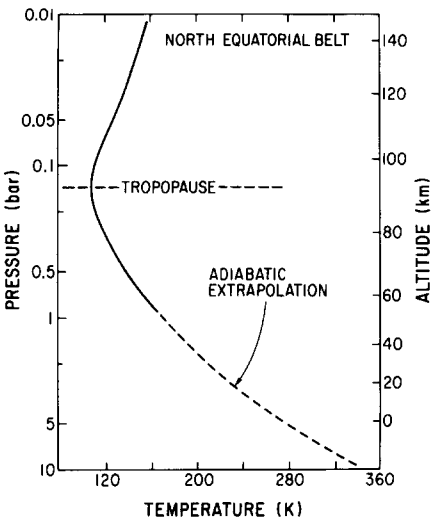

FIG. 2. The temperature–pressure profile for Jupiter's North Equatorial Belt (Kunde *et al.*, 1982) is used to model the central disk observations from the KAO. The temperature at 1 bar is 165 K. The T profile is assumed to follow a dry adiabat for $P > 1$ bar.

value of 250 cm^{-1} used by Kunde *et al.* (1982) in the 5-μm region. We selected a constant value of 50 cm^{-1} to characterize all lines in the 5-μm region. This is probably more realistic than the Kunde *et al.* value (Birnbaum, private communication, 1983). Laboratory measurements of the far-wing profile are clearly needed to define this parameter. We note, however, that our abundance analysis depends on line to continuum ratios near the center of Jupiter's 5-μm window. Consequently, our results are much less sensitive to errors in the Lorentz cutoff parameter than are analyses of data at lower spectral resolution.

4. OVERVIEW

We present an overview of Jupiter's 5-μm spectrum to indicate the principal absorbers as well as to locate the pressure level where most of the absorption takes place. We display in Fig. 1 (top) the airborne spectrum of Jupiter at 5 μm. The shape of the 5-μm window is determined by the far-wing absorption of saturated vibration–rotation bands of NH_3 and PH_3. The long wavelength end of the window is dominated by the ν_4 band of NH_3 with an additional contribution due to the pressure-induced opacity of H_2. The short wavelength end of the 5-μm window is controlled by the ν_1 and ν_3 fundamental bands of PH_3. Absorption lines from 1850 to 1900 cm^{-1} are primarily due to the ν_4 and $2\nu_2$ bands of NH_3 with lines of the latter band extending to 2080 cm^{-1}. Water lines belonging to the ν_2 band occur in the 1900 to 2100 cm^{-1} interval. Phosphine absorbs across much of the 5-μm window; absorption near 1972 cm^{-1} is due to the $2\nu_2$ band, a prominent series of lines centered at 2108 cm^{-1} is due to $\nu_2 + \nu_4$, and a progression of lines of increasing strength from 2150 to 2250 cm^{-1} is due to the ν_1, ν_3, and $2\nu_4$ bands. The ν_2 fundamental of CH_3D dominates the spectrum from 2100 to 2200 cm^{-1}, while the 1-0 fundamental of CO and the ν_3 fundamental of GeH_4 influence the 2050- to 2150-cm^{-1} region. Finally, we report here the first detection of the weak $\nu_3 - \nu_4$ hot band of CH_4 which has absorption features visible in the Jovian spectrum from 1900 to 1935 cm^{-1}.

In Fig. 1 (center) we display the best spectrum calculated by our radiative transfer model for comparison with the observed spectrum of Jupiter. The observations are well matched by the synthetic spectrum, including the slope of the continuum at both ends of the 5-μm window as well as the absolute radiance of the continuum. The agreement of specific spectral features for individual gases is discussed in detail later.

In Fig. 1 (bottom) we indicate the pressure level in the model atmosphere where the gaseous optical depth equals unity as a function of wavenumber across the 5-μm window. The maximum contribution to the thermal emission originates at the indicated pressure level at each wavenumber. Inspection of Fig. 1 shows that most spectral features are formed in the 2- to 5-bar region. We therefore have a set of weighting functions which, in the absence of cloud opacity, sample deep levels in Jupiter's troposphere.

Our radiative transfer model includes a massive absorbing cloud with a normal optical thickness of 2.93 at 5 μm and a base at 2.1 bars, where T = 210 K. The optical thickness was calculated by adding sufficient particle opacity to our gas-only model atmosphere until the calculated radiance at 2080 cm^{-1} matched the observed value in the airborne Jupiter spectrum. The cloud base temperature was inferred by matching observed and calculated values of the continuum radiance at the long and short wavelength ends of Jupiter's 5-μm window. We describe this procedure in detail in Bjoraker *et al.* (1986b).

We used the following criteria to determine the abundance of each of the 5 μm absorbing gases on Jupiter. In Figs. 3 to 11 we compare the observed spectrum of Jupiter from the KAO with a baseline model. This "best fit" was produced after many iterations of gas mole fractions and cloud parameters in the radiative transfer model.

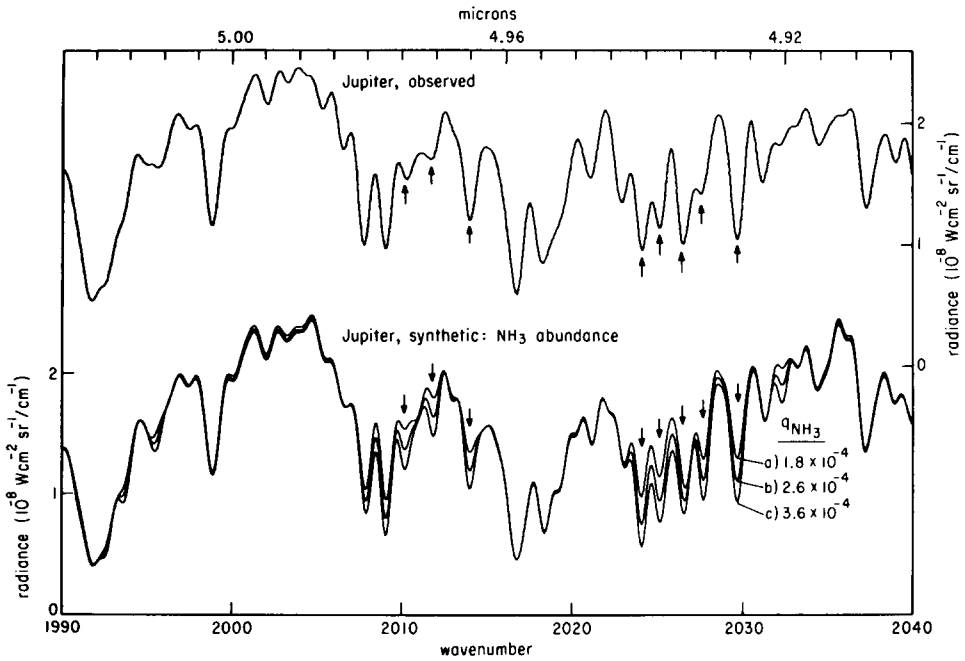

FIG. 3. Jovian NH_3 absorption features between 1990 and 2040 cm^{-1}. The observed spectrum (top) is compared with three synthetic spectra (bottom). Arrows denote the positions of NH_3 transitions. The baseline model in which $qNH_3 = 2.6 \times 10^{-4}$ is shown in trace (b). Synthetic spectra with smaller and larger NH_3 mole fractions are shown in traces (a) and (c), respectively.

We then perturbed one parameter of the baseline model, such as qNH_3,[2] to test its effect on the calculated spectrum. In general, each figure shows the preferred mole fraction in the baseline model, as well as higher and lower values for comparison with the observed data. The absorption lines of the gas of interest are readily identified by visual inspection of the figures since the line to continuum ratio changes dramatically with its abundance. The large number of absorption lines per molecule means that more realistic determinations of mixing ratios should be possible. We now examine each 5-μm absorber individually.

5. INDIVIDUAL MOLECULES

(a) *Ammonia*

It is necessary to probe below levels where condensation and photochemistry take place to determine the global NH_3 abundance on Jupiter. The 2000- to 2100-cm^{-1} portion of Jupiter's spectrum is ideally suited for this task because thermal radiation originates in the 3- to 5-bar pressure range, as indicated in Fig. 1. This is well below both the NH_3 and NH_4SH clouds thought to be present on Jupiter near 0.5 and 2 bars, respectively (Atreya and Romani, 1985). The Q branch and the strong $R1$ and $R2$ lines of the $2\nu_2$ band of NH_3 at 1880, 1920, and 1939 cm^{-1}, respectively, sample atmospheric levels at $P < 2$ bar. However, analysis of the much weaker lines $R6$ through $R10$ between 2007 and 2082 cm^{-1} provides information on the tropospheric nitrogen abundance in the 3- to 5-bar pressure range. These measurements should provide a good test of models which predict an N/H ratio equal to that in the Sun.

The principal absorbers on Jupiter between 1990 and 2090 cm^{-1} are H_2O, PH_3, and NH_3. We have plotted this part of Jupi-

[2] We use the notation qNH_3 to denote the mole fraction of gaseous ammonia in Jupiter's atmosphere.

ter's spectrum in Figs. 3 and 4. We compare Jupiter's airborne spectrum (upper trace) with three synthetic spectra (lower traces) calculated using the radiative transfer model described earlier. The center synthetic spectrum, where $q\mathrm{NH_3} = 2.6 \times 10^{-4}$, represents the best fit to the entire 5-μm spectrum of Jupiter. Plotted on the same scale are synthetic spectra calculated from the same model atmosphere, but for $q\mathrm{NH_3} = 1.8 \times 10^{-4}$ and 3.6×10^{-4}. For each of the three synthetic spectra the $\mathrm{NH_3}$ distribution of Kunde *et al.* (1982) is used for $P <$ 0.7 bar since the 5-μm spectrum is not sensitive to the $\mathrm{NH_3}$ profile above this level in Jupiter's atmosphere. Approximately 30 $\mathrm{NH_3}$ lines are apparent. In particular, the $R7$ manifold near 2025 $\mathrm{cm^{-1}}$ (Fig. 3) and the $R10$ line at 2082 $\mathrm{cm^{-1}}$ (Fig. 4) require a consistent value for $q\mathrm{NH_3}$ of 2.6×10^{-4} in the deep atmosphere. The corresponding global N/H value is 1.45×10^{-4}, or 1.5 times the solar value of Lambert (1978).

We now discuss the probable error in this abundance determination. We used the 15 prominent $\mathrm{NH_3}$ lines denoted by arrows in Figs. 3 and 4 to compare our best synthetic spectrum (trace b) to the observed airborne data. We estimated the lower and upper limits to $q\mathrm{NH_3}$ by visual inspection. The values of $q\mathrm{NH_3}$ used to generate the synthetic spectra shown in traces a and c were chosen to clearly identify the positions of $\mathrm{NH_3}$ absorption features in Figs. 3 and 4. The observed $\mathrm{NH_3}$ lines are in all cases stronger than the calculated lines in trace a and weaker than those of trace c. Profiles a and c represent approximately 2 σ limits to the $\mathrm{NH_3}$ abundance estimated using all 15 $\mathrm{NH_3}$ absorption features. We therefore adopt the value $q\mathrm{NH_3} = (2.6 \pm 0.4) \times 10^{-4}$. We attribute this error primarily to uncertainties in the laboratory $\mathrm{NH_3}$ absorption coefficients. Random noise in the observed spectrum is too small to contribute significantly to our abundance error bar.

Systematic errors are difficult to quantify, but we qualitatively assess their impact on our derived mole fraction. There are many errors that affect the slope of the

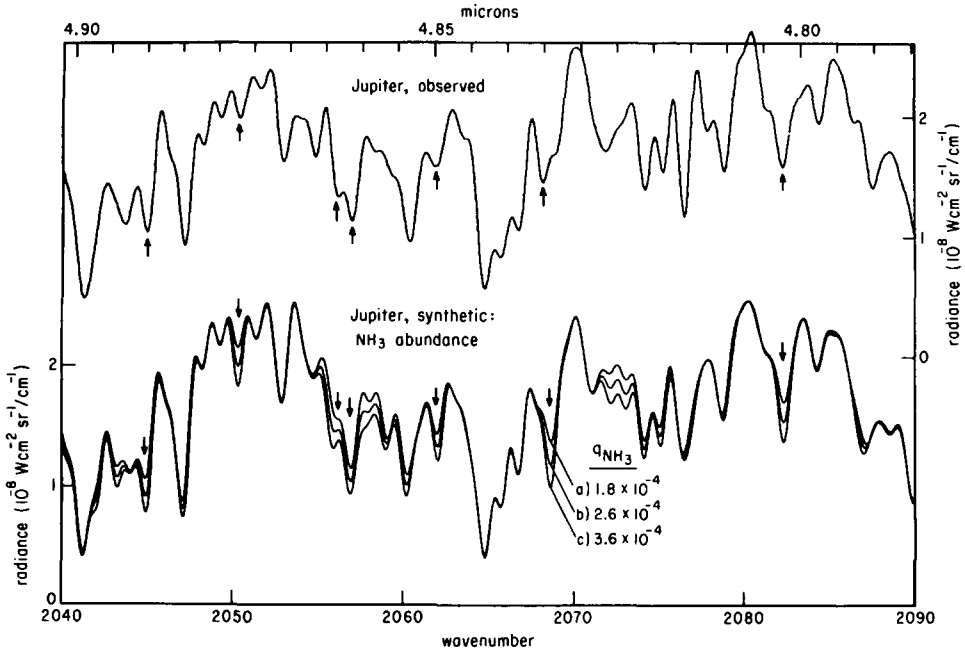

FIG. 4. Same as Fig. 3, but for $\mathrm{NH_3}$ features between 2040 and 2090 $\mathrm{cm^{-1}}$.

continuum, such as (1) uncertainties in the far-wing lineshape of NH_3 and PH_3, (2) the wavelength dependence of cloud opacity, and (3) the absolute flux calibration procedure. These affect the continuum level but not the line to continuum ratio. Since our abundance estimate relies primarily on the line to continuum ratio for individual NH_3 lines, it is quite insensitive to these potential sources of systematic error.

Other types of systematic error could be more serious. The temperature profile is extrapolated along a dry adiabat for $T > 165$ K, as there are currently no direct temperature measurements at levels deeper than 1 bar. Also, uncertainties in the dependence of the Lorentz half width on rotational quantum number and temperature may be a serious problem at 5 μm. This is because the line formation region varies from 1 to 5 bars across the 5-μm window. The abundance inferred from strong lines formed at lower pressures may be different from that derived from weaker lines due to these uncertainties in the molecular data. We have tried to minimize this effect by using only weak lines formed between 3 and 5 bars on Jupiter.

In addition, the line to continuum ratio is affected by cloud opacity. A cold cloud located well above the 5-μm line formation region will attenuate both the line center and continuum radiation equally, thereby preserving the line to continuum ratio that would be present in a cloud-free atmosphere. On the other hand, a warm haze mixed uniformly with the gas at 250 K on Jupiter would attenuate the continuum more than line center, and so would reduce the contrast of the observed lines. We conclude in Bjoraker *et al.* (1986b) from Voyager IRIS data that the main cloud layer is sufficiently cold that the line to continuum ratio of weak 5-μm absorption lines is not significantly altered by overlying clouds.

The NH_3 abundance derived from 5-μm observations is of particular interest because NH_3 is a tracer of many physical and chemical processes occurring in Jupiter's atmosphere. First, 5-μm measurements probe levels of the atmosphere below both the NH_4SH and NH_3 clouds which have depleted the amount of NH_3 in the gas phase by chemical reaction and condensation. These measurements below both cloud layers provide the best global N/H abundance which, in turn, may constrain models of Jupiter's origin. Second, measurements of the partial pressure of NH_3, in combination with an improved temperature–pressure profile of Jupiter's atmosphere, constrain the location of both the NH_4SH and NH_3 clouds in thermochemical equilibrium models. Third, a combination of 5-μm airborne spectra with Voyager IRIS measurements at 45 and 10 μm (Kunde *et al.*, 1982) defines the vertical distribution of NH_3 in Jupiter's troposphere over the extended pressure range from 5 to 0.2 bar. The falloff of gaseous NH_3 measured by Kunde *et al.* (1982) for $P < 1$ bar provides circumstantial evidence that the composition of the cloud near 0.5 bar is NH_3 ice. However, an unambiguous spectroscopic signature of NH_3 ice in Jupiter's infrared spectrum has not been observed (Marten *et al.*, 1981), although a feature may be present at 3 μm (Larson *et al.*, 1984). Finally, the release of latent heat in phase changes at the NH_3 cloud level may be important in atmospheric dynamics.

We compare in Table I our 5-μm estimate of Jupiter's NH_3 abundance to measurements at other wavelengths. Since the abundance of NH_3 is height dependent due to photochemistry and condensation, measurements at wavelengths that sample different levels in Jupiter's atmosphere will yield very different abundances. The only other measurements of Jupiter's NH_3 abundance that apply to pressure levels greater than 2 bars are radio observations at $\lambda > 6$ cm. Marten *et al.* (1980) modeled radio observations at 6 and 11 cm to derive a deep tropospheric NH_3 mixing ratio of 4×10^{-4}, decreasing to 1.3×10^{-4} near the 1-bar level. Higher spatial resolution measurements by de Pater *et al.* (1982) and de Pater

TABLE I

RECENT MEASUREMENTS OF NH_3 ON JUPITER

Transition	Wavelength region	Pressure (bars)	qNH_3	Reference
$2\nu_2$	4.8–5.1 μm	5	$2.6 \pm 0.4 \times 10^{-4}$	This study
?, $5\nu_1$	0.55, 0.65 μm	1	$2.5 \pm 0.9 \times 10^{-4}$	Sato and Hansen (1979)
ν_2	9 μm	0.8	$3.0 \pm 1.5 \times 10^{-4}$	Knacke *et al.* (1982)
Rotation	45 μm	1	$1.8 \times 0.9 \times 10^{-4}$	Kunde *et al.* (1982)
Inversion	1.3 cm	0.7	2×10^{-4}	Klein and Gulkis (1978)
Inversion	1–11 cm	1–6	$(1 - 4) \times 10^{-4}$	Marten *et al.* (1980)
Inversion	6–21 cm	2–10	$(2 - 4) \times 10^{-4}$	de Pater *et al.* (1982)
Inversion	13 cm	1	$2.2 \pm 0.8 \times 10^{-4}$	Lindal *et al.* (1981)

and Massie (1985) using the Very Large Array at 6, 11, and 21 cm also indicate an N/H ratio between 1 and 2 times the solar value.

Numerous measurements have been made of the NH_3 abundance near the 1-bar level on Jupiter. Sato and Hansen (1979) used a two-cloud scattering model to interpret spectra of strong and weak NH_3 bands on Jupiter near 6000 Å. They reported an N/H ratio of 1.5 ± 0.5 times the solar value for the 0.7- to 2-bar region on Jupiter, in excellent agreement with our results for the 5-bar level. Klein and Gulkis (1978) found a solar abundance of nitrogen on Jupiter based on observations at 1 to 2 cm near the inversion band of NH_3. Lindal *et al.* (1981) estimated that $qNH_3 = (2.2 \pm 0.8) \times 10^{-4}$ from radio occultation measurements using the Voyager S band ($\lambda = 13$ cm) radio signal. Kunde *et al.* (1982) analyzed IRIS spectra of the North Equatorial Belt and reported a solar N/H ratio at the 0.8 to 1-bar level. Finally, Knacke *et al.* (1982) found a mixing ratio $[NH_3]/[H_2]$ of $(3.3 \pm 1.7) \times 10^{-4}$ at the 1-bar level. All of these recent observations indicate a tropospheric N/H ratio between 1 and 2 times the value measured in the solar photosphere.

There still is some uncertainty over whether the NH_3 mole fraction changes at the level of the NH_4SH clouds. The infrared, visible, and radio occultation measurements of NH_3 at the 1 bar level described above agree with our NH_3 measurements at 5 bars within the error limits. This would imply that qNH_3 does not change significantly near the 2-bar level of the NH_4SH cloud. Yet ground-based radio observations of Jupiter suggest the opposite conclusion. Marten *et al.* (1980) reported an ammonia mole fraction which drops by a factor of 3 from the 10- to the 2-bar level which they suggest is evidence for a condensed form of nitrogen. De Pater *et al.* (1982) also reported a possible drop in Jupiter's NH_3 abundance by a factor of 2 between 10 and 2 bars. Recently, de Pater and Massie (1985) reported that qNH_3 for Jupiter falls off by perhaps a factor of 5 between the 2- and 1-bar levels. Measurements at 21 cm sample very deep levels ($P = 10$ bars), but the signal-to-noise ratio is lower than in radio observations at shorter wavelengths because nonthermal magnetospheric radiation dominates the atmospheric thermal component. In addition, the presence of other opacity sources, such as H_2O, and uncertainties in the NH_3 lineshape at radio frequencies (de Pater and Massie) affect the interpretation of the radio data. For these reasons the vertical profile of NH_3 in Jupiter's atmosphere inferred from radio observations remains uncertain.

Depending on the sulfur to nitrogen ratio on Jupiter, a modest falloff in the NH_3 abundance would take place as NH_3 reacts with H_2S to form the NH_4SH cloud. Larson *et al.* (1984) set a stringent upper limit to qH_2S on Jupiter for $P < 1$ bar, a result that is consistent with the efficient removal of

sulfur from the gas phase to form an NH_4SH cloud. Using a solar mixing ratio of S/H in the deep atmosphere and the N/H ratio derived here, the resultant drop in the abundance of gaseous NH_3 in forming an NH_4SH cloud would be only about 10%. To distinguish between this prediction of a modest falloff in $q NH_3$ and the much larger drop suggested by the microwave observations, it is necessary to examine the long wavelength end of Jupiter's 5-μm window. Figure 1 shows that the line formation region for ν = 1850 to 1900 cm^{-1} is between 1 and 2 bars. Our baseline model, which uses a constant value of $q NH_3$ between 0.8 and 5 bars, provides an acceptable fit to this region. From this result we conclude that our data are consistent with a modest falloff in NH_3 in this pressure range; a drastic falloff is not required to fit the observations. However, we cannot exclude height dependent NH_3 distributions using presently available data. To derive the vertical distribution of NH_3 more precisely, observations of Jupiter at higher spectral resolution are needed as well as improved molecular parameters for the ν_4 band of NH_3.

(b) Phosphine

Phosphine is an important gaseous absorber across much of Jupiter's 5-μm window. In particular, a prominent series of absorption features centered at 2108 cm^{-1} are due to the $\nu_2 + \nu_4$ vibration–rotation band of PH_3. For $\nu > 2150$ cm^{-1} there is a complex superposition of $2\nu_4$, ν_1, and ν_3 lines whose absorption determines the sharp falloff of the short wavelength end of the 5-μm window. We show in Fig. 1 that all of the PH_3 lines in Jupiter's spectrum from 2100 to 2150 cm^{-1} originate near the 5-bar level, while the 2150- to 2200-cm^{-1} region samples levels between 2 and 5 bars. In Figs. 5 and 6 we compare this part of Jupiter's spectrum to three synthetic spectra with PH_3 mixing ratios of 4×10^{-7}, $7 \times$

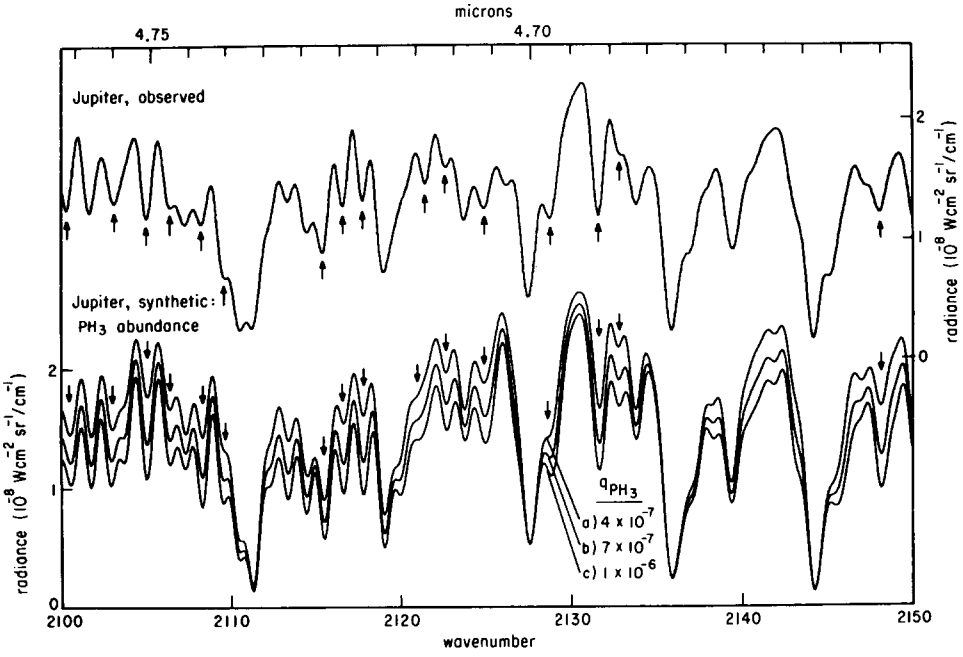

FIG. 5. PH_3 absorption on Jupiter (2100–2150 cm^{-1}). The observed data are compared with the baseline model (trace b) and with spectra (traces a and c) calculated using values of $q PH_3$ bracketing the adopted abundance. Arrows denote PH_3 transitions.

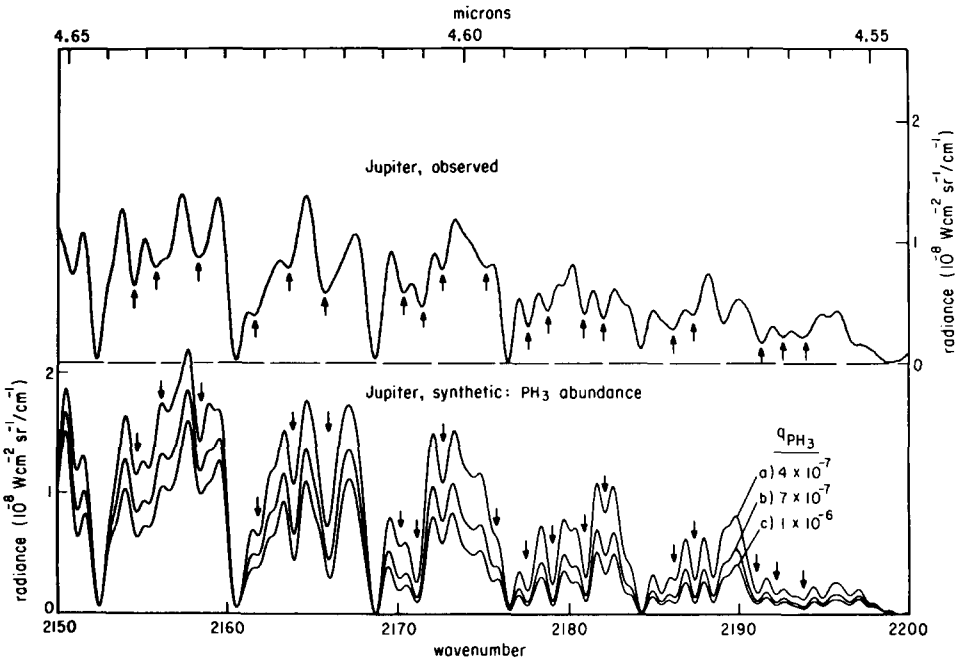

FIG. 6. Same as Fig. 5, but for PH_3 features between 2150 and 2200 cm^{-1}.

10^{-7}, and 1×10^{-6} in the deep atmosphere. The 5-μm spectrum is not sensitive to the distribution of PH_3 for $P < 1$ bar; we adopt the distribution of Kunde *et al.* (1982) for Jupiter's upper troposphere in our model.

In Fig. 5 some 20 PH_3 lines are clearly evident. The agreement between the observed spectrum and the baseline model, curve b, is very good in this spectral region. Therefore, at the 5-bar level $q\mathrm{PH_3} = 7 \times 10^{-7}$. In Fig. 6 we show a transition region of Jupiter's spectrum in which PH_3 and CH_3D lines of increasing strength lead to a rapid decrease of the pressure in the line formation region. Here the agreement between observed and synthetic data is not as good as in Fig. 5; nevertheless, the constant value $q\mathrm{PH_3} = 6 \times 10^{-7}$ provides a reasonable fit to this portion of Jupiter's spectrum. Additional evidence for a value of $q\mathrm{PH_3} = 7 \times 10^{-7}$ comes from features in the 1950- to 2100-cm^{-1} region (Bjoraker, 1985).

We therefore adopt the value $q\mathrm{PH_3} = (7 \pm 1) \times 10^{-7}$ for the 2- to 5-bar region of Jupiter's troposphere. The error estimate is determined by systematic errors in the laboratory absorption coefficients and in the model atmosphere calculation rather than by random errors in the observations. The global P/H ratio becomes $(3.9 \pm 0.6) \times 10^{-7}$. There currently is disagreement concerning the solar abundance of phosphorus. Cameron (1982) cites a solar P/H ratio of 2.44×10^{-7} while Anders and Ebihara (1982) adopt a value of 3.82×10^{-7}. Both compilations refer to measurements of phosphorus in carbonaceous chondrites. A spectroscopic measurement of P/H in the solar photosphere (Pagel, 1977) of 3.16×10^{-7} is intermediate between the meteoritic estimates. Our Jovian P/H ratio is therefore between 1.0 and 1.6 times the solar abundance.

We indicate in Table II some previous PH_3 abundance measurements on Jupiter. These include both Earth-based and Voyager observations at 5 and 10 μm. Phosphine was discovered in absorption at 10

TABLE II

RECENT MEASUREMENTS OF PH_3 ON JUPITER

Transition	Wavelength region (μm)	Pressure (bars)	qPH_3	Reference
$\nu_2 + \nu_4$	4.8	5	$7.0 \pm 1.0 \times 10^{-7}$	This study
ν_4	9.0	1	6×10^{-7}	Ridgway *et al.* (1976)
$\nu_2 + \nu_4$	4.8	5	25 cm-amagat	Larson *et al.* (1977)
ν_1, ν_3	4.5	1–2	4 cm-amagat	Beer and Taylor (1979)
ν_4	9.0	1	$7.5 \pm 1.8 \times 10^{-7}$	Knacke *et al.* (1982)
ν_1, ν_3	4.6	1–4	$6.0 \pm 2.0 \times 10^{-7}$	Kunde *et al.* (1982)
ν_1, ν_3	4.5	1–2	$4.1 \pm 1.5 \times 10^{-7}$	Drossart *et al.* (1982)

μm by Ridgway *et al.* (1976). Larson *et al.* (1977) detected PH_3 at 5 μm and they reported a column abundance of 25 cm-am on Jupiter. They compared room temperature laboratory spectra of PH_3 to the series of prominent Jovian lines near 2100 cm^{-1} in Fig. 5. Beer and Taylor (1979) compared room-temperature PH_3 data to ground-based observations in the 2150- to 2250-cm^{-1} region. They matched the slope of the continuum of the Jovian spectrum with a PH_3 column abundance of 3 to 5 cm-am. The discrepancy between the two reported column abundances is probably due to the difference in the pressure of the line formation region between 2100 and 2200 cm^{-1}. Using a mole fraction $qPH_3 = 7 \times 10^{-7}$, the column abundance of PH_3 above 6 bars is 17 cm-am, versus only 5 cm-am above 2 bars. Because the penetration depth is changing very quickly from 2150 to 2200 cm^{-1}, it is not appropriate to use room-temperature data and a single column abundance to characterize this region. However, at 2100 cm^{-1} the penetration depth does not change rapidly with frequency and the base of the line forming region is coincidentally close to room temperature. This circumstance fortuitously allows the result of Larson *et al.* to agree with the PH_3 abundance obtained here using radiative transfer techniques. Drossart *et al.* (1982) used a radiative transfer model to fit PH_3 in the 2200- to 2240-cm^{-1} region of the Voyager IRIS data. They reported a mixing ratio $[PH_3/H_2] = (4.5 \pm 1.5) \times 10^{-7}$. Unfortunately, the signal-to-noise ratio in this spectral region is only about 3 due to the low flux from Jupiter and the relatively high noise equivalent spectral radiance of the IRIS spectrometer. Knacke *et al.* (1982) reported $[PH_3/H_2] = (8.3 \pm 2.0) \times 10^{-7}$ at the 1-bar level from observations of the ν_4 band at 9 μm. Finally, using a radiative transfer model to fit IRIS data at 4.5 and 9 μm, Kunde *et al.* (1982) reported that $qPH_3 = 6 \times 10^{-7}$ in the 1- to 5-bar region, decreasing to 2×10^{-7} at about the 0.4-bar level. All of these studies suggest that the P/H ratio in the spectroscopically accessible part of Jupiter's atmosphere is at least as large as in the Sun. In particular, our observations suggest that both nitrogen and phosphorus have a common enrichment factor of about 1.5 with respect to the Sun.

Phosphine on Jupiter is of particular interest because of its role as a source of phosphorus, a possible cloud chromophore, and as a tracer of tropospheric convection. The presence of PH_3 at spectroscopically observable levels in Jupiter's atmosphere was not expected from equilibrium thermochemical models. Barshay and Lewis (1978) calculated an equilibrium mole fraction of PH_3 that drops from 4×10^{-7} at 1000 K to less than 10^{-20} at 300 K. Phosphine should be oxidized to P_4O_6 gas in the 800 to 1000 K range and then, for $T <$ 385 K, this product in turn reacts with NH_3 and H_2O to form particles of $NH_4H_2PO_4$.

These calculations assume that O/H = 8.3 $\times$ 10^{-4}, which is the value in the photosphere of the Sun (Lambert, 1978). Some PH_3 could survive to observable levels if the deep atmospheric abundance of H_2O is insufficient to oxidize all of the PH_3. This mechanism could work if the H_2O mole fraction is less than 3/2 that of PH_3. For our value of qPH_3, 7×10^{-7}, the implied upper limit to qH_2O would be 1×10^{-6}. This is well below Jovian H_2O abundance estimates for the deep atmosphere (Kunde *et al.*, 1982; Drossart and Encrenaz, 1982; Bjoraker *et al.*, 1986a) so H_2O depletion is probably not responsible for the observed PH_3 abundance.

The currently accepted explanation for abundant PH_3 on Jupiter, proposed by Prinn and Barshay (1977), is that vertical transport in Jupiter's troposphere is rapid enough to quench chemical reactions that would otherwise destroy PH_3. This same mechanism has also been used to explain the presence of CO and GeH_4 on Jupiter. Prinn and Barshay calculated that an eddy diffusion coefficient $K = 2 \times 10^8$ cm^2 sec^{-1} would be sufficient to transport CO on a time scale shorter than its conversion time to CH_4, the low-temperature form of carbon. Recently, Fegley and Prinn (1983, 1985) studied the kinetics of PH_3 oxidation applied to both Jupiter and Saturn. They concluded that for $K = 2 \times 10^8$ cm^2 sec^{-1} in Jupiter's deep atmosphere, PH_3 oxidation is quenched at 1240 K. This is comparable to the 1100 K quench level obtained for CO by Prinn and Barshay. This corresponds to $P = 600$ bars, or 5 pressure scale heights below the 5-μm line formation region.

The role of phosphorus as a possible cloud chromophore has been investigated both theoretically and experimentally. Prinn and Lewis (1975) proposed that red phosphorus (P_4) might be responsible for the coloration of the Great Red Spot and perhaps of Jupiter's belts as well. They proposed a reaction sequence which can be summarized as

$$PH_3 \rightarrow h\nu \rightarrow PH_2 \rightarrow PH \rightarrow P_2 \rightarrow P_4 \rightarrow P_4(s).$$

Ultraviolet photons with wavelengths between 1800 and 2350 Å produce the intermediate radical PH_2. This product, in turn, may form PH leading to the formation of P_4 along the pathway indicated above. Alternatively, PH_2 may react with itself to form P_2H_4. Another mechanism creating PH_2 is the reaction

$$NH_2 \rightarrow PH_3 \rightarrow NH_3 + PH_2.$$

However, this reaction was found to be very slow at Jovian temperatures (Bosco *et al.*, 1982).

Ferris and Benson (1980) reported that P_2H_4 is the principal intermediate rather than PH in the formation of red phosphorus. At the low temperatures near the tropopause of Jupiter and Saturn P_2H_4 may condense, (Ferris *et al.*, 1984) thus constituting part of a haze layer on these planets. However, this presents a problem for interpreting Jupiter's cloud colors in terms of phosphorus compounds. If solid P_2H_4 has a low vapor pressure at temperatures between 110 and 150 K, it cannot then be photolyzed to produce P_4 at an appreciable rate. Measurements of the vapor pressure of P_2H_4 are needed in this temperature range to determine whether condensation occurs under conditions in Jupiter's upper troposphere.

Recently, Ferris and Khwaja (1985) performed laboratory studies of photolysis of PH_3 at temperatures between 157 and 187 K. They used a 2062-Å iodine lamp to photolyze PH_3 to form P_2H_4. The quantum yield of P_2H_4 formation was found to be independent of temperature and pressure. Condensation of P_2H_4 on the wall of the photolysis cell took place at 157 K. At this temperature the vapor pressure of P_2H_4 was sufficiently high that it slowly converted to an orange-brown material, presumably P_4. However, on Jupiter 2000-Å photons do not penetrate much deeper than 400 mbar (Hord *et al.*, 1979) where the temperature is

near 125 K. It appears that further laboratory studies of PH_3 photolysis will be needed at temperatures colder than those investigated by Ferris and Khwaja in order to reproduce Jovian conditions more closely.

It is difficult to reproduce the visual spectrum of the Great Red Spot in the laboratory and, even if successful, there remains a uniqueness problem. Noy *et al.* (1981) produced P_4 in the laboratory under simulated Jovian conditions and concluded that the visual appearance of the product is usually yellow, not red. However, particles of P_4 about 0.05 μm in size viewed against a white background can reproduce the visual spectrum of the Great Red Spot. Somewhat larger particles are orange while particles larger than 0.5 μm are yellow in appearance. Thus, particle size and viewing geometry are probably just as important as chemical composition in interpreting the colors of Jupiter's clouds. Prinn and Lewis also noted that strong upward mixing with the eddy diffusion coefficient $K > 10^6$ cm^2 sec^{-1} is required to produce the observed coloration.

In summary, there is an adequate supply of phosphine in Jupiter's upper troposphere to manufacture chromophores. Kunde *et al.* (1982) have shown that qPH_3 falls off above the NH_3 cloud, presumably due to photochemistry. Under special conditions that may exist only in selected regions, such as the Great Red Spot, P_4 may be formed. Depending on the particle size, an overall red, orange, or yellow color may result.

(c) *Methane*

Methane is certainly the most thoroughly studied molecule on Jupiter; nevertheless, its abundance is still not known with great certainty. The C/H ratio in Jupiter's atmosphere is of considerable interest as it provides an important observational constraint in models of the formation and subsequent evolution of the outer planets. An estimate of the mixing ratio of CH_4 at deep levels in Jupiter's atmosphere may help distinguish between homogeneous models which predict a solar C/H ratio, or accretion models which predict a substantial enhancement in carbon with respect to the Sun.

We report here the first detection of the very weak $\nu_3 - \nu_4$ hot band of CH_4 in Jupiter's 5-μm spectrum. A hot vibration–rotation band is one in which transitions originate from an excited vibrational quantum state ($v > 0$) rather than from the ground state. The population of the lower vibrational state is very temperature sensitive and it is much smaller than the ground state population at typical planetary temperatures. This band is much weaker than other infrared CH_4 bands and, therefore, indicative of the physical state of Jupiter's deep troposphere.

The presence of a hot band in the atmosphere of a cold outer planet is initially quite surprising. Its existence is a direct consequence of the great depth of line formation in the 5-μm region. We could use this information in two different ways: to deduce the first C/H value from 5-μm data; or to determine precisely the 5-μm line forming region, assuming C/H values from analyses in other wavelength regions. We chose the former approach because knowledge of the global C/H value on Jupiter is very important, and we felt that the 5-μm line formation region is already correctly specified by independent analyses of other 5-μm absorbers, as summarized in Fig. 1.

We have identified six lines in the R branch of the $\nu_3 - \nu_4$ hot band of CH_4 at the following frequencies in Jupiter's spectrum: 1899.7, 1915.6, 1929, 1930.1, 1931.2, and 1935 cm^{-1} (see Fig. 7). The line formation region is between 4 and 6 bars for this portion of Jupiter's 5-μm window. The strongest components of the $R11$ and $R12$ manifolds of the $\nu_3 - \nu_4$ band are evident at 1899.7 and 1915.6 cm^{-1}, respectively. In addition, there are four components of the $R13$ manifold between 1929 and 1935 cm^{-1}. The strong isolated line at 1931.2 cm^{-1} pro-

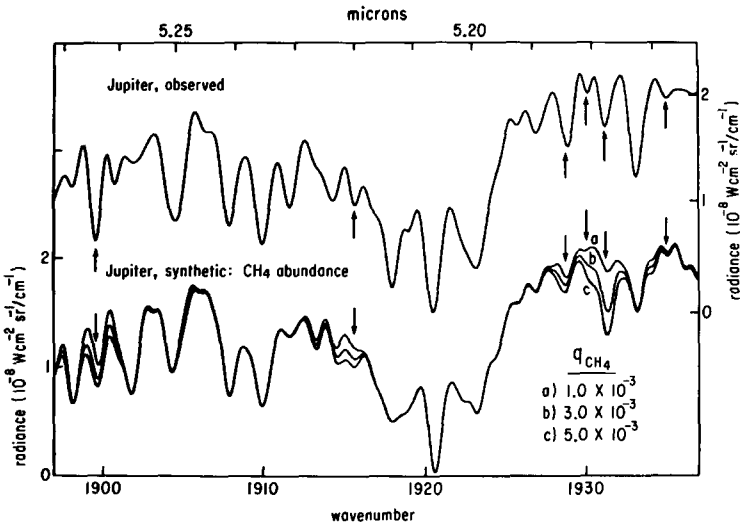

FIG. 7. CH_4 in Jupiter's troposphere. Absorption features between 1897 and 1937 cm^{-1} are indicated in the observed and synthetic spectra. Trace b represents the best fit.

vides the best evidence for the presence of this band in Jupiter's spectrum.

The principal absorbers in this spectral region are H_2O and NH_3. It is especially important to understand the influence of NH_3 absorption because high-J lines of the ν_4 band of NH_3 are adjacent to, or in some cases blended with, the CH_4 lines of interest. Recent improvements in the line positions and strengths of NH_3 (Fink *et al.*, 1983) have given us confidence that the Jovian spectral features discussed here are in fact due to CH_4 and not due to NH_3.

Three synthetic spectra of Jupiter are shown in Fig. 7. Curves a, b, and c represent values for qCH_4 of 1.0×10^{-3}, 3.0×10^{-3}, and 5.0×10^{-3}, respectively. The CH_4 features at 1900, 1929, and 1935 cm^{-1} are blended with NH_3 lines, while the three CH_4 features at 1915.6, 1930.1, and 1931.2 cm^{-1} are relatively isolated lines which show greater sensitivity to changes in the CH_4 abundance in our model. Curve b provides the best overall fit: $qCH_4 = (3.0 \pm 1.0) \times 10^{-3}$. The C/H ratio becomes $(1.7 \pm 0.6) \times 10^{-3}$, or 3.6 ± 1.2 times the solar value of Lambert (1978). The error is primarily due to uncertainty in fitting the line profiles of the CH_4 absorption features at 1930 and 1931 cm^{-1} simultaneously. A larger abundance is required to fit the former feature than that needed to fit the stronger 1931-cm^{-1} line. Thus, our uncertainty in qCH_4 is larger than for the 5-μm absorbers. Higher spectral resolution observations are therefore very desirable to resolve the individual CH_4 components of the $R13$ manifold and to separate them from nearby NH_3 and H_2O lines.

We compare in Table III our C/H ratio to only a few of the many studies of CH_4 on Jupiter that have appeared in the literature. Three basic techniques have been used to calculate CH_4 abundances. The first, and most model dependent, technique is to match both strong and weak lines using a scattering model. Sato and Hansen (1979) used a two-cloud model to fit simultaneously pairs of strong and weak CH_4 bands between 0.543 and 1.10 μm. Buriez and de Bergh (1980) performed a careful analysis of the $3\nu_3$ band of CH_4 at 1.1 μm. They also used a two-cloud model to fit 40 CH_4 lines in a high-resolution spectrum of Jupiter. Another technique developed by Combes and Encrenaz (1979) involves selecting CH_4 and H_2 lines which ideally are formed in the same level of the atmosphere

TABLE III

RECENT C/H DETERMINATIONS FOR JUPITER

CH_4 band	Wavelength region (μm)	Pressure (bars)	(C/H) Jupiter/ (C/H) Sun[a]	Description	Reference
$\nu_3 - \nu_4$	5.2	5.0	3.6 ± 1.2	Airborne IR	This study
$3\nu_3$ + visible	0.5 – 1.1	0.5	2.0 ± 0.4	Scattering model	Sato and Hansen (1979)
$3\nu_3$	1.1	0.5	3.2 ± 1.5	Scattering model	Buriez and de Bergh (1980)
$3\nu_3$ + visible	0.5–1.1	0.5	2.6 ± 1.0	Line ratios	Encrenaz and Combes (1982)
ν_4	8	0.5	2.32 ± 0.18	Voyager IRIS	Gautier and Owen (1983a)
ν_4	8.5	0.8	2.7 ± 0.4	Ground based	Knacke *et al.* (1982)

[a] (C/H) Sun = 4.7×10^{-4} (Lambert, 1978).

and undergo the same scattering processes. They used CH_4 lines in the visible and at 1.1 μm for comparison with the 4–0 S_1 quadrupole line of H_2 at 0.6368 μm.

Another technique relies on measurements in the thermal infrared. Radiative transfer models have been used to synthesize Jupiter's 8-μm spectrum in order to analyze both ground-based and Voyager observations. Gautier *et al.* (1982) analyzed Voyager IRIS spectra of Jupiter in the region near 8 μm where the ν_4 band of CH_4 absorbs. They reported that $[CH_4/H_2] = (1.95 \pm 0.22) \times 10^{-3}$ in the upper troposphere of Jupiter, later revised to $(2.18 \pm 0.18) \times 10^{-3}$ (Gautier and Owen, 1983b). Knacke *et al.* (1982) analyzed ground-based observations of Jupiter at 8.5 μm where radiation originates in the 0.5- to 1-bar region. They reported that $[CH_4/H_2] = (2.5 \pm 0.4) \times 10^{-3}$.

All of these recent studies indicate an enhancement of the Jovian C/H ratio by a factor between 2 and 4. This contradicts earlier beliefs that the atmosphere of Jupiter has an essentially solar composition. This study provides additional independent observational evidence for a significant enhancement of carbon in Jupiter's atmosphere with respect to the Sun. Our measured value of C/H at 5 μm is near the high end of the values in Table III, but still within the error bars. Our CH_4 measurements have the advantage of higher spectral resolution than in the IRIS data used by Gautier *et al.*, and they are less model dependent than the Sato and Hansen and Buriez and de Bergh studies. Overlying clouds may, however, affect the line to continuum ratio of the hot band used in this study. Analysis of the spatial variation of this CH_4 band across Jupiter should be a good test of models of Jupiter's cloud structure such as that proposed by Bjoraker *et al.* (1986b). Our observations of CH_4 pertain to much deeper levels (near 5 bars) than the other measurements cited in Table III, which refer to $P < 1$ bar. However, we do not attribute differences in the C/H ratios summarized in Table III to a height dependent CH_4 distribution because CH_4 does not condense in Jupiter's atmosphere and photochemical destruction of CH_4 takes place only at $P < 1$ mbar in the stratosphere (Strobel, 1983). We conclude from the combined evidence of these six studies that Jupiter's atmosphere is globally enhanced in carbon by about a factor of 3 with respect to the solar photosphere.

(*d*) *Deuterated Methane*

The abundance of deuterium in the atmospheres of the outer planets serves as a tracer of planetary evolution as well as pro-

viding an observational test of cosmological models. Due to Jupiter's large mass and low exospheric temperature, measurements of the present deuterium abundance should be representative of the composition of the solar nebula 4.6 billion years ago. Measurements of the abundance of HD and CH_3D provide information on the fractionation of deuterium between those molecules on Jupiter. The temperature dependence of fractionation may be used to infer an equilibration temperature at the time of Jupiter's formation.

We report here measurements of the ν_2 band of CH_3D in our airborne spectrum of Jupiter. The P-branch of the ν_2 band of CH_3D is responsible for the series of strong absorption lines in the 2100- to 2200-cm^{-1} portion of Jupiter's infrared spectrum in Fig. 1. Twelve J lines are evident in our airborne data. We present the six most prominent lines in Fig. 8: the $P10$ manifold near 2120 cm^{-1} through the $P5$ multiplet near 2160 cm^{-1}. Most of the remaining lines are due to PH_3 and a few weak lines of CO and GeH_4. Reference to Fig. 1 indicates that the base of the line formation region is at 6 bars, with unit optical depth in the cores of the strong CH_3D lines occurring between 1 and 3 bars. Three distributions corresponding to values for qCH_3D of (1, 2, and 3) $\times$ 10^{-7} are included in Fig. 8. The best overall fit is provided by $qCH_3D = (2.0 \pm 0.4) \times 10^{-7}$ (curve b). We have used a constant mole fraction in our model since the abundance of CH_3D is not expected to change with height due to chemistry, condensation, or photolysis in Jupiter's troposphere.

To convert our CH_3D abundance to a D/H ratio the mole fraction of CH_4 and the fractionation factor describing partitioning of deuterium between HD and CH_3D must be known. The D/H ratio by number is given by

$$D/H = qCH_3D/(4fqCH_4),$$

where f is the deuterium fractionation factor and the factor of 4 accounts for the replacement of any one of the four H atoms in CH_4 by one D atom. Beer and Taylor (1978a) report an f value of 1.37 $\pm$ 0.07.

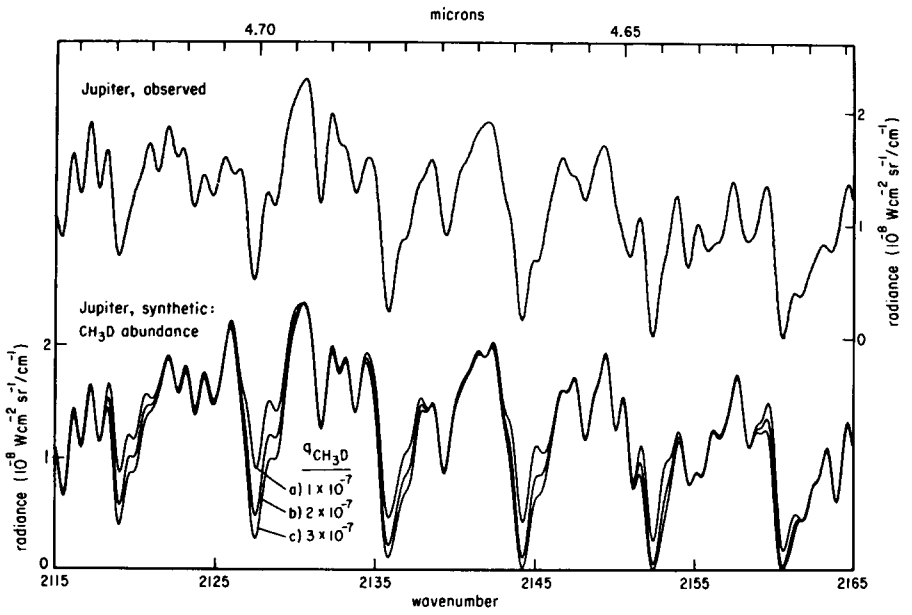

FIG. 8. CH_3D on Jupiter (2115 to 2165 cm^{-1}). Six strong absorption features due to CH_3D are evident by inspection of the three lower traces. Trace b provides the best match to the observed data.

Using our "best-fit" value $qCH_4 = 3.0 \times 10^{-3}$, our D/H ratio becomes $(1.2 \pm 0.5) \times 10^{-5}$. The largest uncertainty is in the CH_4 abundance itself.

We summarize in Table IV the measurements of Jupiter's D/H ratio that have appeared in the literature. Beer and Taylor (1973) first detected CH_3D in ground-based observations of the ν_2 band at 4.7 μm and they acquired higher resolution spectra in 1978. For consistency in comparing D/H values we have converted their column abundance to a mole fraction using the Curtis-Godson approximation. Since the base of the line formation region in our model is at 6 bars, the column abundance of CH_3D must be divided by the hydrogen and helium column abundance at 3 bars. The resulting CH_3D mole fractions are 1.9×10^{-7} and 2.9×10^{-7} for Beer and Taylor's 1973 and 1978 data, respectively. Using Voyager IRIS observations of Jupiter, Drossart *et al.* (1982) inferred that $qCH_3D = 1.8 \times 10^{-7}$ for the region between $-30°$ and $+30°$ latitude, while Kunde *et al.* (1982) reported a value of 3.5×10^{-7} for the Hot Spots in the North Equatorial Belt.

Some of the variation in the CH_3D mole fractions tabulated in Table IV is due to the use of different line intensities for the ν_2 band at 4.7 μm. Chackerian and Guelachvili (1983) accurately measured absolute line intensities for the ν_2 band of CH_3D. We have incorporated these CH_3D parameters as well as improved PH_3 data in our radiative transfer model.

Comparisons of D/H ratios derived from different bands are difficult because, in addition to differences in line strengths and model atmospheres, there is the problem of assuming a C/H ratio and a deuterium fractionation factor. We show in Table IV D/H ratios derived from the measured CH_3D mole fractions using updated estimates for the C/H ratio. For each study in which C/H was derived in the same analysis, we used the reported C/H ratio to calculate a corresponding value for D/H in Table IV. Otherwise, the C/H value reported by Gautier and Owen (1983b) was used (2.3 times solar). In all cases a deuterium fractionation factor of 1.37 (Beer and Taylor, 1978a) was assumed. The D/H ratios derived from CH_3D measurements range from 3.2×10^{-5}

TABLE IV

RECENT MEASUREMENTS OF D/H FOR JUPITER

Molecule	Wavelength (μm)	$qCH_3D \times 10^7$	$\frac{(C/H)\ Jupiter}{(C/H)\ Sun}$	D/H $\times 10^5$	Reference
CH_3D	4.7	2.0 ± 0.4	3.6	1.2 ± 0.5	This study
CH_3D	4.7	$1.9^{+1.1}_{-0.7}$	2.3	$1.8^{+1.0}_{-0.7}$	Beer and Taylor (1973)
CH_3D	4.7	$2.9^{+1.7}_{-1.2}$	2.3	$2.7^{+1.6}_{-1.1}$	Beer and Taylor (1978)
CH_3D	4.5	$1.8^{+1.4}_{-0.9}$	2.3	$1.7^{+1.3}_{-0.9}$	Drossart *et al.* (1982)
CH_3D	4.7, 8.5	$3.5^{+1.0}_{-1.3}$	2.3	$3.2^{+0.9}_{-1.3}$	Kunde *et al.* (1982)
CH_3D	8.7	3.6 ± 0.5	2.7	$3.0^{+1.1}_{-0.8}$	Knacke *et al.* (1982)
HD	0.747	—	—	2.1 ± 0.4	Trauger *et al.* (1973)
HD	0.747	—	—	5.6 ± 1.4	McKellar *et al.* (1976)
HD	0.747	—	—	5.1 ± 0.7	Trauger *et al.* (1977)
HD	0.747	—	2.6	$2.0^{+1.1}_{-0.8}$	Encrenaz and Combes (1982)

(Kunde *et al.*, 1982) to 1.2×10^{-5} (this investigation) with the variation due principally to the measured CH_4 abundance.

An independent approach to calculating Jupiter's D/H ratio is to measure HD and H_2 lines in the reflected solar portion of Jupiter's spectrum. Trauger *et al.* (1973) measured the $P_4(1)$ line of HD at 0.747 μm and the $S_4(1)$ line of H_2 at 0.6368 μm to infer D/H = $(2.1 \pm 0.4) \times 10^{-5}$. Using new laboratory data, this value was revised by McKellar *et al.* (1976) to yield $(5.6 \pm 1.4) \times 10^{-5}$. Trauger *et al.* (1977) remeasured the same HD line with greater accuracy and reported D/H = $(5.1 \pm 0.7) \times 10^{-5}$. Combes and Encrenaz (1979) applied their technique for determining abundance ratios by using the Trauger *et al.* (1977) HD data in conjunction with measurements of a nearby CH_4 line to derive D/C = $(1.0 - 2.7) \times 10^{-2}$. Encrenaz and Combes (1982) used the same technique to derive a C/H ratio for Jupiter that is 2.6 times the Lambert (1978) value for the Sun. Upon combining the two results (D/C and C/H) they deduced that D/H = $(2.0 \pm 1.1) \times 10^{-5}$. Thus, the multiple application of the Combes and Encrenaz method has led to an inferred Jovian D/H ratio which is nearly equal to that derived from CH_3D studies.

In summary, measurements of Jupiter's D/H ratio range from $(1.2 - 5.6) \times 10^{-5}$. Our calculated D/H ratio is at the low end of this range. All of these values have a higher dispersion than do other measurements of Jupiter's composition because the D/H calculation depends on three independent parameters, each of which has its own errors. These are (1) the C/H ratio for Jupiter, (2) the deuterium fractionation factor f, and (3) the mole fraction of either HD or CH_3D. Reference to Table IV indicates that, in general, measurements of the Jovian D/H ratio using CH_3D are smaller than estimates using HD. To reconcile these observations, it may be necessary to revise current ideas of deuterium fractionation in the outer solar system. The deuterium fractionation factor, f, depends upon the temperature of equilibration between H_2 and CH_4 in Jupiter's deep atmosphere. The details of this process are not well understood.

It is interesting to compare the Jovian D/H measurements to values obtained for other solar system objects and the interstellar medium (for a detailed comparison see Kunde *et al.* (1982). Jupiter and Saturn are believed to have retained the deuterium abundance representative of the solar nebula (Hubbard and MacFarlane, 1980). These authors also predicted that Uranus and Neptune should exhibit significant deuterium enhancement due to equilibration at very low temperatures. Observations do not yet exist for Neptune, but measurements of D/H for Saturn range from 2×10^{-5} to 5×10^{-5} (Fink and Larson, 1978; Macy and Smith, 1978) and values for Uranus lie between 3×10^{-5} and 5×10^{-5} (Macy and Smith, 1978; Trafton and Ramsay, 1980). Thus, the observed D/H ratios in the atmospheres of the outer planets are in the $(1–5) \times 10^{-5}$ range. This may be representative of the deuterium abundance in the solar nebula although the mechanisms that enhance deuterium via fractionation are not well understood. Also, the Uranus data raise some questions concerning the equilibration process since the results are in conflict with the Hubbard and MacFarlane prediction of D/H $> 10^{-4}$ for both Uranus and Neptune.

The galactic D/H ratio is between 5×10^{-6} (Vidal-Madjar *et al.*, 1983) and 2×10^{-5} (Bruston *et al.*, 1981). This range overlaps the low end of values observed in the atmospheres of the outer planets. In particular, Jovian D/H ratio is in reasonably good agreement with galactic values. This agreement reinforces expectations that Jupiter's present atmosphere contains a relatively unaltered reservoir of deuterium that is representative of the solar nebula. The cosmological implications of Jupiter's deuterium abundance are discussed in detail by Kunde *et al.* (1982) and Gautier and Owen (1983a).

(e) *Carbon Monoxide*

Carbon monoxide is not expected to be present in observable quantities in Jupiter's atmosphere (Lewis, 1969), yet it was observed in both ground-based observations (Beer, 1975; Beer and Taylor, 1978b) and in airborne spectra (Larson *et al.*, 1978). In this section we compare our airborne spectrum to radiative transfer models of both tropospheric and stratospheric distributions of CO on Jupiter. We have used improved molecular parameters for PH_3, which is the principal absorber in the 2050- to 2150-cm^{-1} region where CO absorbs. These better molecular data and our improved model atmosphere now permit us to make a quantitative comparison between the stratospheric distribution proposed by Beer and Taylor (1978b) and the well-mixed tropospheric profile suggested by Larson *et al.* (1978).

In Figs. 9 and 10 we show the observed spectrum of Jupiter with arrows indicating the positions of eighteen CO lines of the 1-0 vibration–rotation band. Below the observed spectrum are three synthetic spectra corresponding to three possible distributions of CO in Jupiter's atmosphere. Curve a illustrates the effect of setting qCO to zero. Distribution b places CO entirely in the stratosphere with a mixing ratio of 4×10^{-8} above the 110-mbar level at the tropopause. The integrated column abundance is 0.02 cm-am. Curve c is a uniformly mixed distribution of CO for a mole fraction of 1×10^{-9}. The integrated column abundance above the 3- and 6-bar levels is 0.013 and 0.027 cm-am, respectively.

The presence of stratospheric CO in Jupiter's 5-μm spectrum would be indicated by absorption rather than emission lines, as shown by curve b in Figs. 9 and 10. At 5 μm the continuum is formed at deep levels

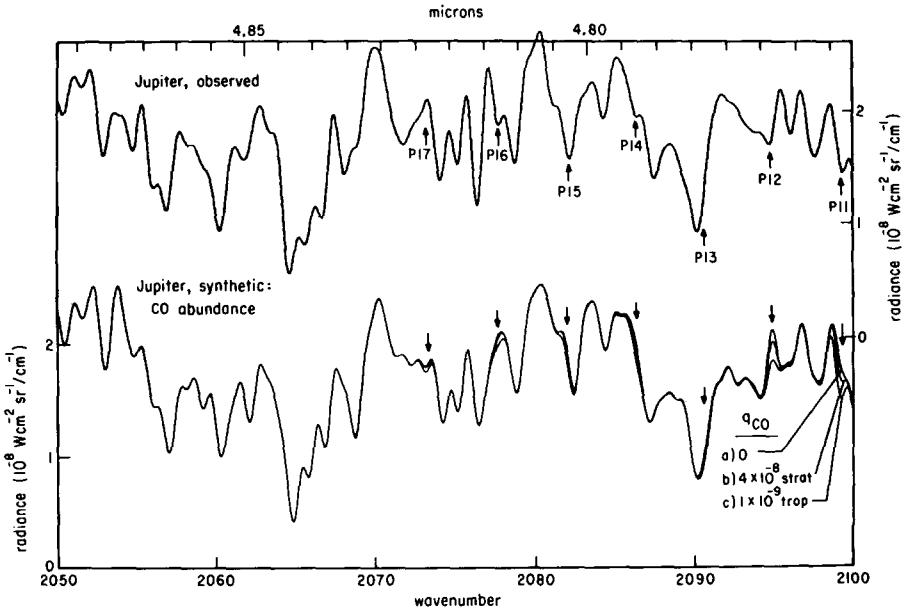

FIG. 9. CO absorption features between 2050 and 2100 cm^{-1}. The planetary data are compared with spectra calculated using three different distributions of CO. Absorption by molecules other than CO is illustrated in trace a where qCO = 0. In trace b CO is concentrated in Jupiter's stratosphere, while in trace c CO is uniformly mixed in the troposphere. Arrows identify each transition of the 1-0 vibration–rotation band. The P11, P14, and P16 transitions are relatively free of blending with other absorbers; they therefore exhibit maximum sensitivity to changes in the CO distribution in the model. The tropospheric distribution (trace c) was adopted for the baseline model.

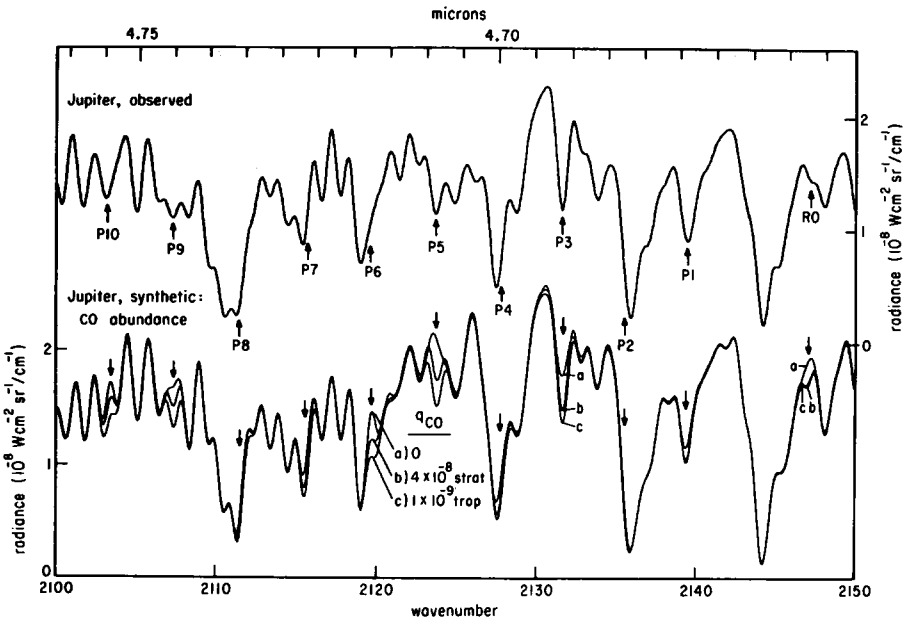

FIG. 10. Same as Fig. 9, but for CO absorption features between 2100 and 2150 cm^{-1}. The most diagnostic spectral features are the relatively isolated $R0$, $P5$, $P6$, and $P9$ transitions of CO.

where $T > 250$ K so, if CO were confined to the stratosphere where $T < 170$ K, absorption lines would be observed. Consequently, in order to distinguish between distribution b, where CO is confined to Jupiter's stratosphere, and curve c, in which CO is uniformly mixed, it is necessary to make a quantitative comparison of line strengths rather than to rely on obvious changes in line profiles.

A comparison between the observed spectrum of Jupiter and distributions a–c is made on a line-by-line basis in Table V. In all cases distribution a can be excluded by comparison with the observed data, confirming that the total absence of CO is inconsistent with the data. Of the eighteen lines from $P17$ to $R0$, six provide no information on distribution due to severe blending with NH_3, PH_3, GeH_4, and CH_3D. Seven lines indicate the presence of CO, but either a stratospheric or tropospheric distribution provides an acceptable fit. For these seven CO lines denoted by BC in Table V, uncertainties in line strengths of other absorbers or the noise level in the observations do not allow one to distinguish between a stratospheric b or tropospheric c CO distribution.

Our evidence for a tropospheric component of CO rests on five lines in Jupiter's spectrum: $P16$, $P14$, $P11$, $P9$, and $P5$. These are isolated lines that exhibit maximum sensitivity to changes of the model abundance of CO. For lines $P11$, $P9$, and

TABLE V

CO 1-0 VIBRATION–ROTATION LINES IN JUPITER'S SPECTRUM

J value	Isolated/ blended[a]	CO profile[b]	J value	Isolated/ blended[a]	CO profile[b]
P17	Bl-NH_3	N	P8	Bl-GeH_4	N
P16	I	C	P7	Bl-PH_3	BC
P15	Bl-NH_3	N	P6	Sh-CH_3D	BC
P14	Sh-H_2O	C	P5	I	C
P13	Bl-H_2O	N	P4	Bl-CH_3D	N
P12	Bl-PH_3	BC	P3	Bl-GeH_4, PH_3	BC
P11	I	C	P2	Bl-CH_3D	N
P10	Bl-PH_3	BC	P1	Bl-PH_3	BC
P9	I	C	R0	Sh-PH_3	BC

[a] I, isolated line; Bl, blend; Sh, shoulder.

[b] A, no CO; B, $qCO = 4 \times 10^{-8}$ in stratosphere only; C, $qCO = 1 \times 10^{-9}$ in troposphere only; BC, CO clearly present, profile B or C possible; N, no information.

$P5$ a uniform value for qCO of $(1.0 \pm 0.3) \times 10^{-9}$ (curve c) provides a significantly better fit to the Jovian spectrum than does the stratospheric distribution (curve b). Lines $P16$ and $P14$ also provide evidence for a tropospheric distribution because these high-J lines are transitions from energy levels populated only at high temperatures. A value for qCO larger than 1×10^{-9} appears to be needed to fit these lines, however. Jovian absorption features at the positions of CO lines between $P5$ and $P16$ are consistently stronger than the stratospheric distribution modeled in curve b. We tried varying the value of qCO in the stratospheric distribution b, but we were unable to fit high- and low-J lines simultaneously. Distribution b was chosen to fit the $R0$ line within error bars. A stratospheric CO mole fraction higher than 4×10^{-8} is required to fit lines $P11$, $P9$, and $P5$, but then the calculated $R0$ line strength would be much stronger than in the observations. In comparison to these difficulties with the stratospheric distributions, the well-mixed CO profile of curve c provides a good fit to ten relatively unblended absorption lines from $P12$ to $R0$, although its mole fraction is too small to match the $P16$ and $P14$ lines. Thus, neither distribution b nor c matches the airborne data exactly, but a tropospheric, well-mixed, distribution with $q\text{CO} = 1 \times 10^{-9}$ provides a better fit to most features in our airborne data than do stratospheric distributions. A height-dependent CO distribution which concentrates most of the CO at warmer tropospheric levels rather than a constant profile may be required to fit the high-J ($P16$, $P14$) and low-J lines simultaneously. We consider this suggestive evidence for a tropospheric component of CO in Jupiter's atmosphere, but a definitive analysis of its vertical distribution must await high altitude observations at higher spectral resolution.

Two disequilibrium mechanisms have been proposed to explain the presence of CO in the observable portion of Jupiter's atmosphere. Prinn and Barshay (1977) suggested that CO is transported from great depth in Jupiter's troposphere on a time scale shorter than the chemical conversion time to reduce CO to CH_4. In thermochemical equilibrium qCO should exceed 10^{-9} only in the deep troposphere where $T >$ 1000 K. The conversion time between the oxidized and reduced forms of carbon depends on temperature because thermal energy is used to break chemical bonds. At the "quench level" the temperature is cold enough that the reaction time equals the time to transport CO convectively to higher, colder altitudes. The location of the quench level and the resulting CO mole fraction above this level depend on the H_2O abundance. This mechanism is attractive because it can also explain the presence of PH_3 and GeH_4 at observable levels in Jupiter's atmosphere.

Alternatively, CO can be produced photochemically from CH_4 provided there is an oxidizing agent such as OH. This process is a source of CO in the Earth's atmosphere. However, ultraviolet photons and oxidizing agents are not located in the same place on Jupiter. Methane photolysis only occurs in the Jovian stratosphere while H_2O is confined to levels deeper than about 2 bars in the troposphere. Consequently, this process can work only if a source of oxygen is introduced into the Jovian stratosphere. Two sources have been suggested. Prather *et al.* (1978) proposed that ablation of meteoroids could supply the necessary oxygen while Strobel and Yung (1979) suggested that the Galilean satellites inject oxygen atoms into the Jovian magnetosphere which, in turn, are ionized, diffuse inward, and penetrate to the mesopause level in Jupiter's atmosphere. Voyager observations of oxygen in the Io plasma torus (Bridge *et al.*, 1979; Broadfoot *et al.*, 1979) as well as Pioneer observations of the meteoroid flux at Jupiter (Humes, 1976) lend support to an extra-Jovian source of oxygen. Strobel (1983) estimated the oxygen source rate that is required to produce the observed CO column abundance. He concluded that ab-

lation of meteoroids can supply enough oxygen, but the Galilean satellite source requires an infall rate near the upper limits of current measurements. Both external sources introduce oxygen at about the 1-μbar level on Jupiter. Subsequent photochemistry, principally via the reaction

$$OH + CH_3 \rightarrow CO + 2H_2,$$

would convert each oxygen atom to a CO molecule. See Strobel (1983) for a detailed discussion of the photochemistry of oxygen compounds on Jupiter.

In summary, theoretical frameworks exist to explain either a preferentially stratospheric distribution of CO fed from an external source of oxygen, or a uniformly mixed tropospheric distribution sustained by rapid vertical convection. Our analyses of CO, PH_3, and GeH_4 collectively support the convective transport mechanism proposed by Prinn and Barshay (1977). Our value of qCO of 1×10^{-9} implies an eddy diffusion coefficient $K = 2 \times 10^8$ cm^2 sec^{-1} in Jupiter's deep atmosphere, according to Fig. 2 in Prinn and Barshay. This value of K is in agreement with estimates derived from measurements of Jupiter's heat flux.

(*f*) *Germane*

Germane has been identified in two independent observations of Jupiter's 5-μm spectrum. Fink *et al.* (1978) first detected GeH_4 by comparing room temperature laboratory data to the same airborne spectrum of Jupiter that we are using in this study. Kunde *et al.* (1982) and Drossart *et al.* (1982) found evidence for GeH_4 in Voyager 1 IRIS spectra of Jupiter. All of these studies have relied on one absorption feature in Jupiter's spectrum—the strong Q-branch of the ν_3 band of GeH_4 at 2111 cm^{-1}. We report here the identification of three additional GeH_4 absorption features as well as suggestive evidence for another five spectral features. We also study the 2111-cm^{-1} absorption feature in detail in order to separate quantitatively the contributions of four Jovian molecules having known absorptions near this frequency.

Germanium has five naturally occurring isotopes with atomic weights of 70, 72, 73, 74, and 76. The terrestrial isotopic percentages are 20.7, 27.5, 7.7, 36.4, and 7.7, respectively. Lepage *et al.* (1981) measured the line parameters for all five isotopic species for both the ν_1 and ν_3 bands of GeH_4. Unfortunately, these data are not available in machine-readable form. Consequently, we were not able to use the Lepage *et al.* data in our radiative transfer calculations, but we did use them qualitatively to estimate isotopic line splittings, for example. We used the spectroscopic parameters for the ν_3 band of $^{74}GeH_4$ to generate synthetic spectra because molecular data exist only for this isotopic species in the GEISA line compilation (Husson *et al.*, 1982). The intensity for the ν_3 band of GeH_4 was normalized to the laboratory value for the sum of all five isotopic species. Hence the absolute line strengths for $^{74}GeH_4$ were 1/(0.364), or 2.75 times the correct value, and the other isotopic species were omitted. The isotopic splitting for the ν_3 band is between 1 and 2 cm^{-1} between the lightest and heaviest isotope. This is large compared to our resolution (0.5 cm^{-1}). Thus, in principle, isotopic abundances may be determined in the future when better molecular data are available.

We display the 2100- to 2150-cm^{-1} region of Jupiter's airborne spectrum at the top of Fig. 11. The three synthetic spectra shown below the observations correspond to three different abundances of $^{74}GeH_4$. In curve a the GeH_4 abundance is set to zero. This synthetic spectrum shows the contribution of CO, PH_3, and CH_3D to Jupiter's complex spectrum in this wavelength region. We display in curves b and c synthetic spectra corresponding to values for $q^{74}GeH_4$ of 2.5×10^{-10} and 7.0×10^{-10}, respectively. We illustrate the effect of isotope splitting of the ν_3 band of GeH_4 in Fig. 11 by marking the positions of the P-branch and R-branch lines with an arrow and a hor-

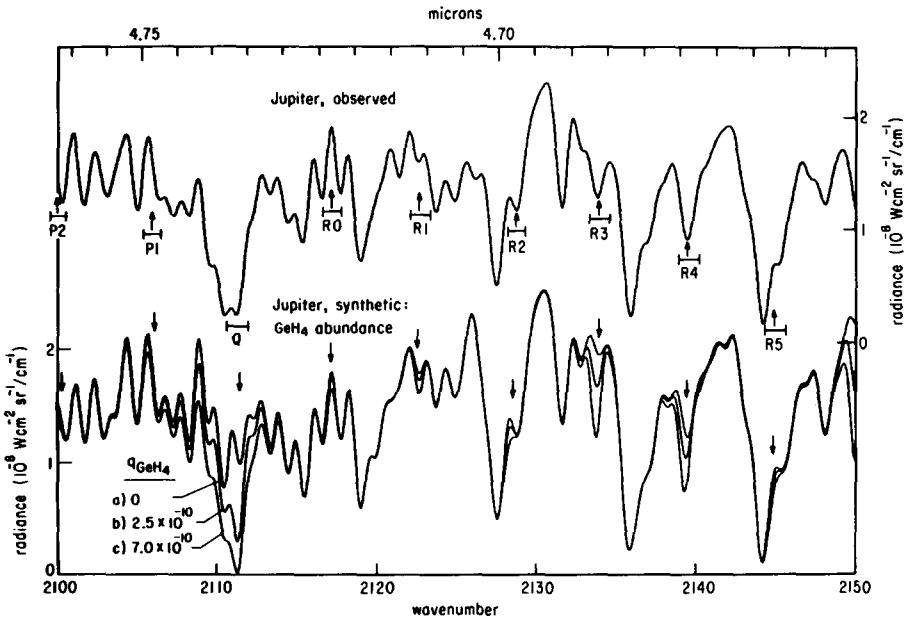

FIG. 11. GeH_4 absorption between 2100 and 2150 cm^{-1}. The frequencies of the ν_3 transitions for the isotopic forms $^{70}GeH_4$ to $^{76}GeH_4$ are indicated by bars; the arrows denote the positions for the $^{74}GeH_4$ isotopic species. The mole fractions used to calculate spectra in traces b and c refer only to the mole fraction of $^{74}GeH_4$; the total GeH_4 abundance is obtained by multiplying by 2.75. The R3 transition at 2134 cm^{-1} is evident in the observations. The complex feature at 2110 to 2112 cm^{-1} is discussed in the text.

izontal bar. The arrow marks the position of the $^{74}GeH_4$ absorption feature, while the length of the bar estimates the spread in absorption between the lightest and heaviest isotopic forms of GeH_4 using data in Lepage *et al.*

In Fig. 11 we present evidence for the presence of GeH_4 in Jupiter's atmosphere. The prominent absorption between 2110 and 2112 cm^{-1} is much stronger in the observed spectrum than in curve a, where $qGeH_4 = 0$. Clearly, absorption by CO, PH_3, and CH_3D alone does not quantitatively match the Jupiter spectrum; therefore, an additional absorber is required. The synthetic spectra in curves b and c, calculated by adding $^{74}GeH_4$ to the model, provide a much better fit to the observations; however, neither spectrum provides a perfect match to this complex feature. We emphasize that our model includes absorption by only the ν_3 band of $^{74}GeH_4$, the only isotopic form for which we have molecular line parameters. We argue below that the apparent disagreement between the synthetic and observed spectra at 2110 cm^{-1} in Fig. 11 is due to the omission in our model of the spectroscopic parameters for the ν_1 band of GeH_4. To test this idea, we need an independent estimate of the Jovian GeH_4 abundance using other GeH_4 absorption features.

We describe below the evidence for two new absorption features due to GeH_4 in Jupiter's 5 μm spectrum. The most prominent of these features is the $R3$ multiplet of GeH_4 at 2134 cm^{-1} in Fig. 11. Curve a shows that absorption due to other molecules is small at this frequency. Curve c has too much GeH_4, while the baseline model shown in curve b matches the observed feature fairly well. The second new feature is the $R6$ manifold at 2150 cm^{-1}, the best evidence for which is in the ground-based

high-resolution (0.1 cm^{-1}) observations of Jupiter of Beer and Taylor (1978a). In their Fig. 1 they presented a 5-μm synthetic spectrum of Jupiter which included absorption due to CH_3D on Jupiter and to H_2O and CO in the Earth's atmosphere. We may now confidently assign PH_3 and GeH_4 to additional features in their Jovian spectrum that were not accounted for by their model. The feature due to the $R3$ multiplet of GeH_4 at 2134 cm^{-1} is quite prominent in their data, while the $R6$ feature is blended with PH_3 even at their resolution of 0.1 cm^{-1}.

There is additional evidence for GeH_4 absorption at five other frequencies. Jovian absorption features at the positions of the $R4$ line shown in Fig. 11 as well as the $P7$, $P4$, $P3$, and $R7$ vibration–rotation lines of the ν_3 band (see Bjoraker, 1985) all require some GeH_4 absorption in the model to fit the airborne data.

We now return to the complex absorption feature at 2111 cm^{-1} in Jupiter's spectrum. This feature is actually a superposition of absorption by four different molecules. The composite spectrum in Fig. 6 of Fink *et al.* (1978) shows that Jovian CO, CH_3D, and GeH_4 all contribute to the observed planetary feature. Phosphine absorbs here as well. We identify the following absorption lines in the interval between 2109 and 2112 cm^{-1}: the $P8$ line of the 1-0 band of CO, the $P11$ multiplet of the ν_2 band of CH_3D, three unassigned rotation lines of the $\nu_2 + \nu_4$ band of PH_3, the Q branch of the ν_3 band of GeH_4, and the Q branch of the ν_1 band of GeH_4.

Our inclusion of the Q branch of the ν_1 band of GeH_4 in this list identifies the last new GeH_4 transition that we are reporting here. Germane is a tetrahedral molecule like CH_4 and so from symmetry considerations the ν_1 band is "forbidden." However, Lepage *et al.* identified many weak absorption lines of the ν_1 band in their laboratory spectra. They noted that these lines are perturbation-allowed ν_1 transitions because the energy difference between the ν_1 and ν_3 vibration modes of GeH_4 is very small. The strength of the Q branch of ν_1 is enhanced because all five isotopic forms of GeH_4 absorb at the same frequency (2110.71 cm^{-1}). The absorption in the much stronger ν_3 Q branch is spread out between 2110.73 cm^{-1} for $^{76}GeH_4$ to 2112.03 cm^{-1} for $^{70}GeH_4$. These positions are listed in Table I of Lepage *et al.*

We have to examine the Jovian 2111-cm^{-1} feature carefully to find the barely resolved signatures of both Q branches of GeH_4 (ν_1 and ν_3). The observed Jovian feature displays two blended components at 2110.5 and 2111.3 cm^{-1}, respectively. The synthetic spectra denoted by curves b and c were calculated using spectroscopic parameters for $^{74}GeH_4$ only. A value for $q^{74}GeH_4$ of 2.5×10^{-10} is sufficient to fit the 2111.3 cm^{-1} feature while the larger abundance of distribution c ($q^{74}GeH_4 = 7.0 \times 10^{-10}$) is required to fit the 2110.5-cm^{-1} feature. We attribute this discrepancy to absorption by the ν_1 Q branch at 2110.71 cm^{-1}, which is present in the observed Jovian spectrum but not in the synthetic data. We anticipate that the addition of the ν_1 line parameters to our model will permit one value of $q^{74}GeH_4$, distribution b, to fit both components of the GeH_4 absorption feature at 2111 cm^{-1}. This conclusion is supported by the agreement between curve b and the observed data for the $R3$ and $R6$ lines. Distribution c is too strongly absorbing to match these features at 2134 and 2150 cm^{-1}. A rigorous test of this conclusion will require the use of line parameters for the ν_1 and ν_3 bands for all five isotopic forms of GeH_4.

Our inferred mole fraction for all isotopic forms of GeH_4 on Jupiter is $(7^{+4}_{-2}) \times 10^{-10}$, assuming terrestrial values of the relative isotopic abundances. The corresponding Ge/H ratio is 3.9×10^{-10}, which is 0.1 times the value in $C1$ chondrites (Cameron, 1982) that is thought to characterize the solar nebula and the bulk composition of Jupiter. Our inferred GeH_4 mole fraction is in very close agreement with the three previous estimates of its abundance in Jupiter's atmosphere. Fink *et al.* (1978) estimated that

$q\mathrm{GeH_4} = 6 \times 10^{-10}$, Kunde *et al.* (1982) inferred $q\mathrm{GeH_4} = 7 \times 10^{-10}$, and Drossart *et al.* (1982) obtained $[\mathrm{GeH_4}]/[\mathrm{H_2}] = 1.0 \times 10^{-9}$.

Germane should not be observable at all in Jupiter's atmosphere. Barshay and Lewis (1978) calculated that in thermochemical equilibrium $\mathrm{GeH_4}$ should react in the deep troposphere with $\mathrm{H_2S}$ and $\mathrm{H_2O}$ to form GeS and GeO. The presence of $\mathrm{GeH_4}$ at temperatures of 200 to 300 K in Jupiter's upper troposphere therefore lends strong additional support to the disequilibrium convective transport model of Prinn and Barshay (1977), which we discussed earlier in connection with our analyses of Jovian $\mathrm{PH_3}$ and CO.

6. SUMMARY

We have presented a compositional analysis of Jupiter's troposphere that used radiative transfer techniques to model airborne observations of Jupiter at high spectral resolution in the 5-μm region. The results characterize the 2- to 6-bar level of Jupiter's atmosphere in which the derived elemental abundances should represent global values on Jupiter. Our tropospheric composition is summarized in Table VI. Of the nine entries, six molecules are analyzed in detail in this paper, $\mathrm{H_2O}$ is presented in a separate publication (Bjoraker *et al.*, 1986a), and the Voyager $\mathrm{H_2}$ and He results are included for completeness. The observed mole fractions in Table VI are compared to values predicted by chemical equilibrium models. Our principal results are summarized below.

(1) Most abundances deviate significantly from expectations based upon an atmospheric model assuming solar composition and chemical equilibrium.

(2) Our clearly enhanced C/H and N/H values, and the depleted O/H value, probably relate to Jupiter's origin. The implications of these abundance ratios are discussed in more detail in Bjoraker *et al.* (1986a).

TABLE VI

SUMMARY OF THE TROPOSPHERIC COMPOSITION OF JUPITER FROM 5-μm AIRBORNE OBSERVATIONS

Molecule	Jovian mole fraction		Solar value	Enhancement over solar value	Comments
	Observed	Predicted			
$\mathrm{H_2}$	0.90 ± 0.02	0.88	0.88[a]	1.0	Gautier *et al.* (1981)
He	0.10 ± 0.02	0.12	0.12[a]	1.0	Gautier *et al.* (1981)
$\mathrm{CH_4}$	$3.0 \pm 1.0 \times 10^{-3}$	8.3×10^{-4}	8.3×10^{-4}[b]	3.6 ± 1.2	
$\mathrm{NH_3}$	$2.6 \pm 0.4 \times 10^{-4}$	1.7×10^{-4}	1.7×10^{-4}[b]	1.5 ± 0.2	
$\mathrm{H_2O}$	$4.0 \pm 1.0 \times 10^{-6}$	1.5×10^{-3}	1.5×10^{-3}[b]	$2.7 \pm 0.7 \times 10^{-3}$	Upper troposphere (2–4 bars)
	$3.0 \pm 2.0 \times 10^{-5}$	1.5×10^{-3}	1.5×10^{-3}[b]	$2.0 \pm 1.4 \times 10^{-2}$	Lower troposphere (6 bars)
$\mathrm{PH_3}$	$7.0 \pm 1.0 \times 10^{-7}$	$<10^{-30}$	4.4×10^{-7}[a]	1.6 ± 0.2	Disequilibrium species
			6.9×10^{-7}[c]	1.0 ± 0.1	
$\mathrm{CH_3D}$	$2.0 \pm 0.4 \times 10^{-7}$				D/H = 1.2×10^{-5}
CO	$1.0 \pm 0.3 \times 10^{-9}$	$<10^{-18}$			Disequilibrium species
$\mathrm{GeH_4}$	$7.0\ ^{+4.0}_{-2.0} \times 10^{-10}$	$<10^{-20}$	7.9×10^{-9}[a]	$8.9\ ^{+5.0}_{-2.5} \times 10^{-2}$	Disequilibrium species

[a] Cameron (1982).
[b] Lambert (1978).
[c] Anders and Ebihara (1982).

(3) Our D/H ratio in Jupiter is comparable to that measured in the interstellar medium.

(4) The unexpected presence of PH_3, GeH_4, and CO in Jupiter's upper troposphere can be satisfactorily explained by rapid convective transport from very deep levels. There remain, however, uncertainties in the reaction rates of phosphorus and germanium compounds under Jovian conditions.

(5) The distribution of gaseous NH_3 in the 1- to 5-bar region is consistent with only modest conversion of NH_3 to condensates (i.e., NH_4SH).

(6) The abundant PH_3 molecule throughout Jupiter's troposphere may contribute to Jupiter's colors through photochemical conversion to elemental phosphorus.

(7) Our observations of a hot band of CH_4 on Jupiter reinforces previous conclusions that absorption lines in Jupiter's 5-μm spectrum form in deep, warm atmospheric levels. Our measurement of an enhanced C/H value at these deep levels strongly suggests that this enhancement is global.

(8) The presence of GeH_4 in Jupiter's atmosphere is now confirmed with multiple spectroscopic features.

(9) The distribution of CO in Jupiter appears to be well mixed, but stratospheric distributions cannot be completely eliminated with presently available data.

(10) We found no compelling evidence in our analysis for previously undetected trace constituents in Jupiter's atmosphere. At a resolution of 0.5 cm^{-1} all Jovian spectral lines in the 5-μm region are consistent with spectra of the molecules listed in Table VI.

(11) Much more information is potentially available from remote spectroscopic studies of Jupiter's atmosphere at 5 μm. For example, a number of partially resolved absorption features in Jupiter's spectrum, such as at 2078 cm^{-1} in Fig. 9, are not well matched by our model calculations. Conversely, some planetary absorptions predicted by our model, such as at 1902 and 1939 cm^{-1} in Fig. 1, do not appear prominently, or even at all, in Jupiter's observed spectrum. These differences may be due to several factors: unidentified trace constituents in Jupiter's atmosphere, inadequacies in the molecular parameters such as line intensities, or incomplete specification of Jupiter's vertical atmospheric structure in the model. Each of these possibilities can be critically examined when new Earth-based planetary spectra at higher spatial and spectral resolution are acquired, but only if accompanied by laboratory studies that allow more realistic numerical simulations of the atmosphere of the outer planets.

APPENDIX

Molecular Spectroscopic Parameters

We present in Table VII a summary of the molecular line parameters used to generate infrared synthetic spectra of Jupiter. The vibration–rotation bands of seven Jovian absorbers are listed. Band intensities were calculated by summing the strengths of individual lines over the specified wavenumber interval. The Lorentz pressure broadening coefficient is also indicated. The tabulated value is a weighted average of the coefficients for H_2-broadened and He-broadened molecules using the helium mole fraction measured by Gautier *et al.* (1981).

The line parameters for the $\nu_3 - \nu_4$ hot band of CH_4 were obtained from the GEISA spectroscopic compilation (Husson *et al.*, 1986) based on an analysis by Hilico *et al.* (1985). Pressure broadened widths for CH_4 are from Fox and Jennings (1985). The molecular parameters for the ν_2 band of CH_3D were generated using symmetric rotor theory. Line strengths are from Chackerian and Guelachvili (1983). We list the intensity of the P, Q, and R branches of the ν_2 band separately in Table VII; only the P-branch data were used in our Jupiter analysis.

TABLE VII

SUMMARY OF MOLECULAR DATA FOR JOVIAN 5-μm ABSORBERS

Gas	Band	ν_{min} (cm^{-1})	ν_{max} (cm^{-1})	Line count	Band intensity 296 K (cm^{-1}/cm-amagat)	($x - H_2 + He$) (cm^{-1} atm^{-1})
CH_4	$\nu_3 - \nu_4$	1474	1994	2003	5.33×10^{-2}	0.066
CH_3D	$\nu_2 P$	2029	2193	210	5.62	0.071
	$\nu_2 Q$	2181	2200	210	6.16	0.071
	$\nu_2 R$	2207	2359	231	9.96	0.071
	ν_2	2029	2359	651	2.17×10^{1}	0.071
NH_3	ν_4^s	1204	1998	801	5.46×10^{1}	0.068
	ν_4^a	1229	2056	818	5.42×10^{1}	0.068
	$2\nu_2^a$	1219	1967	362	5.73×10^{-1}	0.068
	$2\nu_2^s$	1541	2154	359	2.10×10^{-1}	0.068
PH_3	—	1926	2162	621	3.86	0.068
	—	2162	2184	36	5.67	0.068
	ν_1	2184	2446	410	1.36×10^{2}	0.068
	ν_3	2184	2446	827	4.67×10^{2}	0.068
H_2O	ν_2	640	2822	1806	2.79×10^{2}	0.08
^{12}CO	1-0	1968	2267	79	2.64×10^{2}	0.07
GeH_4	ν_3	1937	2225	824	1.10×10^{3}	0.09

The molecular parameters for NH_3 came from two sources. The GEISA spectroscopic data bank (Husson *et al.*, 1982) contains parameters for both the ν_4 and $2\nu_2$ bands. The GEISA line strengths for NH_3 at 5 μm are systematically too strong so we acquired new laboratory spectra at 0.3 cm^{-1} resolution using a one-pass 40-m absorption cell at the Lunar and Planetary Lab. Using these spectra we applied line by line correction factors to the GEISA NH_3 line strengths for both the ν_4 and $2\nu_2$ bands between 1825 and 2154 cm^{-1}. In some cases the observed line strengths are factors of 10 to 100 smaller than the GEISA values.

The molecular parameters for PH_3 were obtained from three sources. Room-temperature measurements of PH_3 line positions and strengths for the 1926- to 2162-cm^{-1} region were from Goldman (1980). This data set alone does not give the temperature dependence of these PH_3 lines. We therefore acquired 5-μm spectra of PH_3 at 0.3-cm^{-1} resolution at both 195 and 300 K. Lower state energies were inferred on a line-by-line basis. Three bands are evident: the $2\nu_2$ band is centered near 1972 cm^{-1}, the $\nu_2 + \nu_4$ band is very prominent at 2108 cm^{-1}, and the $2\nu_4$ band is responsible for low energy lines in the 2150- to 2200-cm^{-1} interval. This latter interval also contains high-energy lines of ν_1 and ν_3 whose band centers are near 2300 cm^{-1}. The molecular constants for the ν_1 and ν_3 bands of PH_3 obtained by Baldacci *et al.* (1980) reside on the GEISA line atlas (Husson *et al.*, 1982); however, no data are available for the $2\nu_4$ band. We roughly accounted for the influence of the $2\nu_4$ band by adjusting the line strengths and lower state energies of the GEISA ν_1 and ν_3 lines until synthetic PH_3 spectra agreed with lab data at both 195 and 300 K. This is provisional until a thorough analysis of PH_3 in this region becomes available (Tarrago, 1985, private communication).

The molecular parameters for H_2O and CO are from the AFCRL Atmospheric Line Parameters Compilation (McClatchey *et al.*, 1973). The molecular parameters for the ν_3 band of GeH_4 are from the GEISA line atlas. A major limitation is that only lines of the $^{74}GeH_4$ isotope are present on this atlas. Finally, molecular hydrogen is an

important absorber not shown in Table VII. Absorption coefficients were calculated for H_2 using the theory developed by Birnbaum and Cohen (1976) and the lab measurements of Bachet *et al.* (1983). A discussion of the use of these lab data to calculate the temperature dependence of H_2 absorption coefficients at 5 μm is given in Bjoraker (1985).

ACKNOWLEDGMENTS

The authors thank K. Fox for help in the identification of CH_4 in our Jupiter data, D. Gautier and J. Hornstein for useful discussions on hydrogen opacity, U. Fink for assistance in the acquisition of NH_3 and PH_3 laboratory spectra, and D. Hunten and W. B. Hubbard for their comments regarding the manuscript. We also thank R. Hanel, B. Conrath, W. Maguire, J. Pearl, R. Samuelson, M. Flasar, and J. Pirraglia of the Voyager IRIS team for their help in the analysis of the IRIS data. Thanks are due to J. Tingley and L. Mayo for their assistance with the Goddard spectrum synthesis program and K. Denomy for the preparation of the numerous figures that appear here. This research was supported by NASA Grant NAG2-206 and by NASA's Graduate Student Researchers Program.

REFERENCES

ANDERS, E., AND M. EBIHARA (1982). Solar-system abundances of the elements. *Geochim. Cosmochim. Acta* **46,** 2363–2380.

ATREYA, S. K., AND P. N. ROMANI (1985). Photochemistry and clouds of Jupiter, Saturn, and Uranus. In *Planetary Meteorology* (G. E. Hunt, Ed.), pp. 17–68. Cambridge Univ. Press, Cambridge.

BACHET, G., E. R. COHEN, P. DORE, AND G. BIRNBAUM (1983). The translational-rotational absorption spectrum of hydrogen. *Can. J. Phys.* **61,** 591–603.

BALDACCI, A., V. M. DEVI, K. N. RAO, AND G. TARRAGO (1980). Spectrum of phosphine at 4 to 5 μm: Analysis of ν_1 and ν_3 bands. *J. Mol. Spectrosc.* **81,** 179–206.

BARSHAY, S. S., AND J. S. LEWIS (1978). Chemical structure of the deep atmosphere of Jupiter. *Icarus* **33,** 593–611.

BEER, R. (1975). Detection of carbon monoxide in Jupiter. *Astrophys. J.* **200,** L167–L169.

BEER, R., AND F. W. TAYLOR (1973). The abundance of CH_3D and the D/H ratio in Jupiter. *Astrophys. J.* **179,** 309–327.

BEER, R., AND F. W. TAYLOR (1978a). The D/H and C/H ratios in Jupiter from the CH_3D phase. *Astrophys. J.* **219,** 763–767.

BEER, R., AND F. W. TAYLOR (1978b). The abundance of carbon monoxide in Jupiter. *Astrophys. J.* **221,** 1100–1109.

BEER, R., AND F. W. TAYLOR (1979). Phosphine absorption in the 5-μm window of Jupiter. *Icarus* **40,** 189–192.

BIRNBAUM, G., AND E. R. COHEN (1976). Theory of lineshape in pressure-induced absorption. *Can. J. Phys.* **54,** 593–602.

BJORAKER, G. L. (1985). The gas composition and vertical cloud structure of Jupiter's troposphere derived from five micron spectroscopic observations. Ph.D. Dissertation, University of Arizona.

BJORAKER, G. L., H. P. LARSON, AND V. G. KUNDE (1986a). The abundance and distribution of water vapor in Jupiter's atmosphere. *Astrophys. J.*, in press.

BJORAKER, G. L., V. G. KUNDE, AND H. P. LARSON (1986b). The vertical cloud structure of Jupiter's lower troposphere, in preparation.

BOSCO, S. R., W. D. BROBST, D. F. NAVA, AND L. J. STIEF (1982). Kinetics of the reaction of NH_2 with phosphine and implications for Jovian atmospheric modeling. *Bull. Am. Astron. Soc.* **14,** 722.

BRIDGE, H. S., J. W. BELCHER, A. J. LAZARUS, J. D. SULLIVAN, R. L. MCNUTT, F. BAGENAL, J. D. SCUDDER, E. C. SITTLER, G. L. SISCOE, V. M. VASYLIUNAS, C. K. GOERTZ, AND C. M. YEATES (1979). Plasma Observations near Jupiter: initial results from Voyager 1. *Science* **204,** 987–991.

BROADFOOT, A. L., M. J. S. BELTON, P. Z. TAKACS, B. R. SANDEL, D. E. SHEMANSKY, J. B. HOLBERG, J. M. AJELLO, S. K. ATREYA, T. M. DONAHUE, H. W. MOOS, J. L. BERTAUX, J. E. BLAMONT, D. F. STROBEL, J. C. MCCONNELL, A. DELGARNO, R. GOODY, AND M. B. MCELROY (1979). Extreme ultraviolet observations from Voyager 1 encounter with Jupiter. *Science* **204,** 979–982.

BRUSTON, P., J. AUDOUZE, A. VIDAL-MADJAR, AND C. LAURENT (1981). Physical and chemical fractionation of deuterium in the interstellar medium. *Astrophys. J.* **243,** 161–169.

BURIEZ, J. C., AND C. DEBERGH (1980). Methane line profiles near 1.1 micron as a probe of the Jupiter cloud structure and C/H ratio. *Astron. Astrophys.* **83,** 149–162.

CAMERON, A. G. W. (1982). Elemental and nuclidic abundances in the solar system. In *Essays in Nuclear Astrophysics* (C. A. Barnes, D. D. Clayton, and D. N. Schramm, Eds.), pp. 23–43. Cambridge Univ. Press, Cambridge.

CHACKERIAN, C., AND G. GUELACHVILI (1983). Direct retrieval of lineshape parameters: Absolute line intensities for the ν_2 band of CH_3D. *J. Mol. Spectrosc.* **97,** 316–330.

COMBES, M., AND T. ENCRENAZ (1979). A method for the determination of abundance ratios in the outer planets—Application to Jupiter. *Icarus* **39,** 1–27.

DE PATER, I., S. KENDERDINE, AND J. R. DICKEL (1982). Comparison of the thermal and nonthermal radiation characteristics of Jupiter at 6, 11, and 21 cm with model calculations. *Icarus* **51,** 25–38.

DE PATER, I., AND S. T. MASSIE (1985). Models of the millimeter–centimeter spectra of the giant planets. *Icarus* **62,** 143–171.

DROSSART, P., AND T. ENCRENAZ (1982). The abundance of water on Jupiter from the Voyager IRIS data at 5 μm. *Icarus* **52,** 483–491.

DROSSART, P., T. ENCRENAZ, V. KUNDE, R. HANEL, AND M. COMBES (1982). An estimate of the PH_3, CH_3D, and GeH_4 abundances on Jupiter from the Voyager IRIS data at 4.5 μm. *Icarus* **49,** 416–426.

ENCRENAZ, T., AND M. COMBES (1982). On the C/H and D/H ratios in the atmospheres of Jupiter and Saturn. *Icarus* **52,** 54.

FEGLEY, B., JR., AND R. G. PRINN (1983). Chemical probes of Saturn's deep atmosphere. *Lunar Planet. Sci. Conf.* **14,** 189–190.

FEGLEY, B., JR., AND R. G. PRINN (1985). Equilibrium and nonequilibrium chemistry of Saturn's atmosphere: Implications for the observability of PH_3, N_2, CO, and GeH_4. *Astrophys. J.* **299,** 1067–1078.

FERRIS, J. P., AND R. BENSON (1980). Diphosphine is an intermediate in the photolysis of phosphine to phosphorus and hydrogen. *Nature* **285,** 156–157.

FERRIS, J. P., A. BOSSARD, AND H. KHWAJA (1984). Mechanism of phosphine photolysis: Application to Jovian atmospheric photochemistry. *J. Am. Chem. Soc.* **106,** 318–324.

FERRIS, J. P., AND H. KHWAJA (1985). Laboratory simulations of PH_3 photolysis in the atmospheres of Jupiter and Saturn. *Icarus* **62,** 415–424.

FINK, U., AND H. P. LARSON (1978). Deuterated methane observed on Saturn. *Science* **201,** 343–345.

FINK, U., H. P. LARSON, G. L. BJORAKER, AND J. R. JOHNSON (1983). The NH_3 spectrum in Saturn's 5 micron window. *Astrophys. J.* **268,** 880–888.

FINK, U., H. P. LARSON, AND R. R. TREFFERS (1978). Germane in the atmosphere of Jupiter. *Icarus* **34,** 344–354.

FOX, K., AND D. JENNINGS (1985). Measurements of nitrogen-, hydrogen-, and helium-broadened widths of methane lines at 9030–9120 cm^{-1}. *J. Quant. Spectrosc. Radiat. Transfer* **33,** 275–280.

GAUTIER, D., B. CONRATH, R. HANEL, V. KUNDE, A. CHEDIN, AND N. SCOTT (1981). The helium abundance of Jupiter from Voyager. *J. Geophys. Res.* **86,** 8713–8720.

GAUTIER, D., B. BEZARD, A. MARTEN, J. P. BALUTEAU, N. SCOTT, A. CHEDIN, V. KUNDE, AND R. HANEL (1982). The C/H ratio in Jupiter from the Voyager infrared investigation. *Astrophys. J.* **257,** 901–912.

GAUTIER, D., AND T. OWEN (1983a). Cosmological implications of helium and deuterium abundances on Jupiter and Saturn. *Nature* **302,** 215–218.

GAUTIER, D., AND T. OWEN (1983b). Cosmogonical implications of elemental and isotopic abundances in atmospheres of the giant planets. *Nature* **304,** 691–694.

GOLDMAN, A. (1980). Stratospheric molecular parameters study, University of Denver.

HILICO, J. C., M. LOETE, AND L. R. BROWN (1985). Line strengths of the $\nu_3 - \nu_4$ band of methane. *J. Mol. Spectrosc.* **111,** 119–137.

HORD, C. W., R. A. WEST, K. E. SIMMONS, D. L. COFFEEN, M. SATO, A. L. LANE, AND J. T. BERGSTRALH (1979). Photometric observations of Jupiter at 2400 Angstroms. *Science* **206,** 956–959.

HUBBARD, W. B., AND J. J. MACFARLANE (1980). Theoretical predictions of deuterium abundances in the Jovian planets. *Icarus* **44,** 676–682.

HUMES, D. H. (1976). The Jovian meteoroid environment. In *Jupiter* (T. Gehrels, Ed.), pp. 1052–1067. University of Arizona Press, Tucson.

HUSSON, N., A. CHEDIN, N. A. SCOTT, I. COHEN-HALLALEH, AND A. BERROIR (1982). La banque de donnees GEISA. Note Interne du Laboratoire de Meteorologie Dynamique 116.

HUSSON, N., A. CHEDIN, N. A. SCOTT, D. BAILLY, G. GRANER, N. LACOME, A. LEVY, C. ROSSETTI, G. TARRAGO, C. CAMY-PEYRET, J. M. FLAUD, A. BAUER, N. MONNANTEUIL, J. C. HILICO, G. PIERRE, M. LOETE, J. P. CHAMPION, L. S. ROTHMAN, L. R. BROWN, G. ORTON, P. VARANASI, C. P. RINSLAND, M. A. H. SMITH, AND A. GOLDMAN (1986). The GEISA Spectroscopic Line Parameters Data Bank in 1984. *Ann. Geophys.* **4,** 2, 185–190.

KLEIN, M. J., AND S. GULKIS (1978). Jupiter's atmosphere: Observations and interpretation of the microwave spectrum near 1.25 cm wavelength. *Icarus* **35,** 44–60.

KNACKE, R. F., S. J. KIM, S. T. RIDGWAY, AND A. T. TOKUNAGA (1982). The abundances of CH_4, CH_3D, NH_3, and PH_3 in the troposphere of Jupiter derived from high resolution 1100–1200 cm^{-1} spectra. *Astrophys. J.* **262,** 388–395.

KUNDE, V. G. (1982). Voyager IRIS measurements of the Jovian atmosphere. In *Vibrational–Rotational Spectroscopy for Planetary Atmospheres* (M. J. Mumma, K. Fox, and J. Hornstein Eds.), pp. 387–405. NASA Conf. Pub. 2223.

KUNDE, V. G., AND W. C. MAGUIRE (1974). Direct integration transmittance model. *J. Quant. Spectrosc. Radiat. Transfer* **14,** 803–817.

KUNDE, V., R. HANEL, W. MAGUIRE, D. GAUTIER, J. P. BALUTEAU, A. MARTEN, A. CHEDIN, N. HUSSON, AND N. SCOTT (1982). The tropospheric gas composition of Jupiter's North Equatorial Belt (NH_3, PH_3, CH_3D, GeH_4, H_2O) and the Jovian D/H isotopic ratio. *Astrophys. J.* **263,** 443–467.

LAMBERT, D. L. (1978). Element abundances in the solar photosphere. VIII. Revised abundances of car-

bon, nitrogen and oxygen. *Mon. Not. R. Astron. Soc.* **182,** 249.

LARSON, H. P., D. S. DAVIS, R. HOFMANN, AND G. L. BJORAKER (1984). The Jovian atmospheric window at 2.7 microns: A search for H_2S. *Icarus* **60,** 621–639.

LARSON, H. P., AND U. FINK (1975). Infrared Fourier spectrometer for laboratory use and for astronomical studies from aircraft and ground-based telescopes. *Appl. Opt.* **14,** 2085–2095.

LARSON, H. P., U. FINK, AND R. R. TREFFERS (1978). Evidence for CO in Jupiter's atmosphere from airborne spectroscopic observations at 5 microns. *Astrophys. J.* **219,** 1084–1092.

LARSON, H. P., U. FINK, R. TREFFERS, AND T. N. GAUTIER (1975). Detection of water vapor on Jupiter. *Astrophys. J.* **197,** L137–L140.

LARSON, H. P., R. R. TREFFERS, AND U. FINK (1977). Phosphine in Jupiter's atmosphere: The evidence from high altitude observations at 5 microns. *Astrophys. J.* **211,** 972–979.

LEPAGE, P., J. P. CHAMPION, AND A. G. ROBIETTE (1981). Analysis of the ν_3 and ν_1 infrared bands of GeH_4. *J. Mol. Spectrosc.* **89,** 440–448.

LEWIS, J. S. (1969). Observability of spectroscopically active compounds in the atmosphere of Jupiter. *Icarus* **10,** 393–401.

LINDAL, G. F., G. E. WOOD, G. S. LEVY, J. D. ANDERSON, D. N. SWEETNAM, H. B. HOTZ, B. J. BUCKLES, D. P. HOLMES, P. E. DOWNS, V. R. ESHLEMAN, G. L. TYLER, AND T. A. CROFT (1981). The atmosphere of Jupiter: An analysis of the Voyager radio occultation measurements. *J. Geophys. Res.* **86,** 8721–8727.

MACY, W., JR., AND W. H. SMITH (1978). Detection of HD on Saturn and Uranus, and the D/H ratio. *Astrophys. J.* **222,** L73–L75.

MARTEN, A., R. COURTIN, D. GAUTIER, AND A. LACOMBES (1980). Ammonia vertical density profiles in Jupiter and Saturn from their radioelectric and infrared emissivities. *Icarus* **41,** 410–422.

MARTEN, A., D. ROUAN, J. P. BALUTEAU, D. GAUTIER, B. J. CONRATH, R. A. HANEL, V. KUNDE, AND R. SAMUELSON (1981). Study of the ammonia ice cloud layer in the equatorial region of Jupiter from the infrared interferometric experiment on Voyager. *Icarus* **46,** 233–248.

MCCLATCHEY, R. A., W. S. BENEDICT, S. A. CLOUGH, D. E. BURCH, R. F. CALFEE, K. FOX, L. S. ROTHMAN, AND J. S. GARING (1973). AFCRL-TR-73-0096.

MCKELLAR, A. R. W., W. GOETZ, AND D. A. RAMSAY (1976). The rotation–vibration spectrum of HD: Wavelength and intensity measurements of the 3-0, 4-0, 5-0, and 6-0 electric dipole bands. *Astrophys. J.* **207,** 663–670.

NOY, N., M. PODOLAK, AND A. BAR-NUN (1981). Photochemistry of phosphine and Jupiter's Great Red Spot. *J. Geophys. Res.* **86,** 11,985–11,988.

PAGEL, B. E. J. (1977). Solar abundances: A new table (October 1976). In *Physics and chemistry of the Earth 11* (L. H. Ahrens, Ed.), pp. 79–80. Pergamon, Oxford.

PRATHER, M. J., J. A. LOGAN, AND M. B. MCELROY (1978). Carbon monoxide in Jupiter's upper atmosphere: An extraplanetary source. *Astrophys. J.* **223,** 1072–1081.

PRINN, R. G., AND S. S. BARSHAY (1977). Carbon monoxide on Jupiter and implications for atmospheric convection. *Science* **198,** 1031–1034.

PRINN, R. G., AND J. S. LEWIS (1975). Phosphine on Jupiter and implications for the Great Red Spot. *Science* **190,** 274–276.

RIDGWAY, S. T., L. WALLACE, AND G. R. SMITH (1976). The 800-1200 inverse centimeter absorption spectrum of Jupiter. *Astrophys. J.* **207,** 1002–1006.

SAARI, J. M., R. W. SHORTHILL, AND D. F. WINTER (1972). The sunlit lunar surface II: A study of far infrared brightness temperatures. *The Moon* **5,** 179–199.

SATO, M., AND J. E. HANSEN (1979). Jupiter's atmospheric composition and cloud structure deduced from absorption bands in reflected sunlight. *J. Atmos. Sci.* **36,** 1133–1167.

STROBEL, D. F. (1983). Photochemistry of the reducing atmospheres of Jupiter, Saturn, and Titan. *Int. Rev. Phys. Chem.* **3,** 145–176.

STROBEL, D. F., AND Y. L. YUNG (1979). The Galilean satellites as a source of CO in the Jovian upper atmosphere. *Icarus* **37,** 256–263.

TERRILE, R. J., AND R. F. BEEBE (1979). Summary of historical data: Interpretation of the Pioneer and Voyager cloud configurations in a time-dependent framework. *Science* **204** 948–951.

TRAFTON, L., AND D. A. RAMSAY (1980). The D/H ratio in the atmosphere of Uranus: Detection of the R5(1) line of HD. *Icarus* **41,** 423–429.

TRAUGER, J. T., F. L. ROESLER, N. P. CARLETON, AND W. A. TRAUB (1973). Observation of HD on Jupiter and the D/H ratio. *Astrophys. J.* **184,** L137–L141.

TRAUGER, J. T., F. L. ROESLER, AND M. E. MICKELSON (1977). The D/H ratios on Jupiter, Saturn, and Uranus based on new HD and H_2 data. *Bull. Am. Astron. Soc.* **9,** 516.

VIDAL-MADJAR, A., C. LAURENT, C. GRY, P. BRUSTON, R. FERLET, AND D. G. YORK (1983). The ratio of deuterium to hydrogen in interstellar space. *Astron. Astrophys.* **120,** 58–62.